

NON-HYPERBOLIC RIGHT-ANGLED COXETER GROUPS
WITH Menger CURVE BOUNDARY

by

Cong He

A Dissertation Submitted in
Partial Fulfillment of the
Requirements for the Degree of

Doctor of Philosophy
in Mathematics

at

The University of Wisconsin-Milwaukee
August 2023

ABSTRACT

NON-HYPERBOLIC RIGHT-ANGLED COXETER GROUPS WITH MENGER CURVE BOUNDARY

by

Cong He

The University of Wisconsin–Milwaukee, 2023
Under the Supervision of Professor Craig Guilbault

We find a class of simplicial complexes as nerves of non-hyperbolic right-angled Coxeter groups, with boundary homeomorphic to the Menger curve. The nerves are triangulations of compact orientable surfaces with boundary. In particular, the nerves are non-graphs.

© Copyright by Cong He, 2023
All rights Reserved

TABLE OF CONTENTS

List of figures	v
List of notations	viii
Acknowledgements	ix
1 Introduction	1
1.1 Overview	1
1.2 Organization	3
2 CAT(0) spaces and groups	5
2.1 CAT(0) spaces	5
2.2 δ -hyperbolic spaces	8
2.3 Examples of group boundaries	9
2.3.1 Sierpiński carpet and Menger curve	9
2.3.2 Pontryagin surface as the boundary of right-angled Coxeter group . .	11
3 The geometry of RACGs	14
3.1 Coxeter groups	14
3.2 Davis complexes	15
3.3 Visual boundaries of Coxeter groups	16
4 Triangulation	18
4.1 Assumptions	18
4.2 Construction of the triangulation	19

5	More properties of Davis complex and Coxeter group	21
5.1	Disjointness in the Davis complex	21
5.2	Disjointness in the visual boundary	24
5.3	Special property of Coxeter groups	28
6	Nullity and density	30
6.1	Properties of geodesic segments	30
6.2	Nullity property	32
7	Locally nonplanar property	36
7.1	Notations	36
7.2	Proof of the locally nonplanar property	37
8	No local cut point	42
8.1	C_{pq} is null	43
8.2	Small B_k inclusion	45
8.3	p_0 is not a local cut point	46
8.3.1	Case 1: $p_0 \in \mathcal{P} \setminus \bigcup_{k=1}^{\infty} B_k$	46
8.3.2	Case 2: $p_0 \in B_{k_0}$ for some k_0	49
9	Other properties of $\partial_{\infty}\Sigma_{N_0}$	51
9.1	Path connected and locally path connected	51
9.2	Visual boundary is 1-dimensional	51
9.3	Completion of the main theorem	52
10	Closing comments and open questions	53
	Bibliography	55

LIST OF FIGURES

2.1	CAT(0) inequality.	6
2.2	Comparison triangle.	8
2.3	The Sierpiński carpet.	10
2.4	The Menger curve.	10
2.5	Pontryagin surface.	12
3.1	Cubification.	16
4.1	Dranishnikov subdivision of a 2-simplex.	19
4.2	“Poison pill” subdivision.	20
5.1	$g_1H_a^+ \cap g_2H_a^+ = \emptyset$	23
5.2	Rays intersect the wall gh_a	25
5.3	The interiors of $\partial_\infty(g_iH_a^+)$ do not intersect.	26
5.4	The boundary of $\partial_\infty(g_2H_a^+)$ does not intersect with the interior of $\partial_\infty(g_1H_a^+)$	26
6.1	$\tilde{G}_{1,\hat{g}}K$ retracts onto $\partial B(x_0, n)$ and $\Pi_n(\tilde{G}_{1,\hat{g}}K) \subseteq B_{\frac{1}{n}}(\xi(n))$	34
7.1	Davis complex Σ_{N_1} : 2-dimensional.	38
7.2	Davis complex Σ_{N_0} : 2-dimensional.	39
7.3	Davis complex Σ_{N_1} : 3-dimensional.	40
7.4	Davis complex Σ_{N_0} : 3-dimensional.	41
8.1	The path goes into and out of Pontryagin disk.	43
8.2	$\{A_{pq}\}_{p,q}$ is null.	44

8.3	B'_k s with $diam(B_k) \leq \frac{\delta}{3}$ are included in U	46
8.4	The purple path goes into the Pontryagin disks.	47
8.5	Push the path segments in B'_k s out.	48
8.6	Case 2: $p_0 \in \partial B_{k_0}$	49
8.7	Reroute the path l	50

LIST OF NOTATIONS

- N : the abstract simplicial complex corresponding to a flag triangulation of a closed surface.
- $K = \text{cone}(N')$ is called the chamber, N' denotes the barycentric subdivision of N .
- $N_0 := N - a, N_1 := N - (a \cup b)$.
- $V_N :=$ vertex set of N .
- L_b : the link of b .
- W_{L_b} : group generated by the vertices of L_b .
- $\mathcal{T}_{N_0,b}$: a special transversal of W_{N_0} for W_{L_b} , i.e.
 $\mathcal{T}_{N_0,b} := \{g' : g' \text{ is the unique minimum length element in coset } gW_{L_b}\}.$
 $\mathcal{T}_{N_0,b}^+ := \{g \in \mathcal{T}_a \mid \ell(ga) > \ell(g)\}.$
- $h_{v_i} := \bigcup_{g \in W_{L_{v_i}}} gP_{v_i}$, P_{v_i} is a panel, and h_{v_i} is sometimes called a wall, see Chapter 3. The wall separates Σ_N into two components, denote the closure of the component without the fundamental chamber by $H_{v_i}^+$, and $H_{v_i}^+ = \bigcup_h \{hK : \ell(v_i h) < \ell(h)\}.$
- gH_a^+ : the translation of H_a^+ by $g \in \mathcal{T}_{N_0,a}$, where
 $\mathcal{T}_{N_0,a}$: transversal of W_{N_0} for W_{L_a} , i.e.
 $\mathcal{T}_{N_0,a} := \{g' : g' \text{ is the unique minimum length element in a coset } gW_{L_a}\}.$
- For any convex set U , denote by $\partial_\infty U$ the geodesic equivalent class in U .
- $\Pi_\delta(\xi)$: the projection of ξ onto $\partial B(x_0, \delta)$.
- $U_{\Pi_\delta(\xi)}$: a neighborhood of $\Pi_\delta(\xi)$ in $\partial B(x_0, \delta)$.
- $\ell(g)$ is the length of any reduced representation of g .
- $In(g) := \{v \in V_N \mid \ell(gv) < \ell(g)\}$, and $Out(g) := \{v \in V_N \mid \ell(gv) > \ell(g)\}.$

ACKNOWLEDGEMENTS

First and foremost, I would like to thank my advisor, Craig Guilbault, who exposed me to the field of Geometric Group and Geometric Topology, and introduced me such a nice topic for my dissertation; without his help, the completeness is unimaginable. Thank him for guiding me for many years including the summer breaks, enduring my naive questions and ignorance, also thank him for helping me modify the writing of the dissertation. His dedication in academic research influenced me and will encourage me to be a good scholar. Beyond academics, he gave me lots of helpful life advice.

I also would like to thank the other dissertation committee members Professors Chris Hruska, Boris Okun, Jonah Gaster and Kevin McLeod for their thoughtful comments on my manuscript and insightful questions during my defense. Special thanks go to Professors Boris Okun and Chris Hruska for many times of individual discussion with them; Professors Jonah Gaster, Chris Hruska and Boris Okun for their criticism about my presentations given in the seminars. Their advice improved my dissertation.

Many thanks go to Professor Jeb Willenbring and the staff working at the front desk of the main office.

I want to thank my fellow graduate students at UWM for their help and friendship. Especially, I would like to thank Arka Banerjee, Daniel Gulbrandsen, Prayagdeep Parija, William Braubach, Joseph Paulson, Ashani Dasgupta and Daniel Noelck.

Finally, I would like to express my deep gratitude to my wife. She has put up with the long nights and anxiety that accompanied the graduate school. Without her strong support, I could not imagine I can persist in to today.

Chapter 1

Introduction

1.1 Overview

In [30], Świątkowski gave a necessary and sufficient condition for a hyperbolic Coxeter group with planar nerve to have Sierpiński curve as its Gromov boundary. And hyperbolic right-angled Coxeter groups with Gromov boundary as Menger curve were studied by Daniel Danielski [7]. Recently, Danielski and Świątkowski gave complete characterizations (in terms of nerves) of the word hyperbolic Coxeter groups whose Gromov boundary is homeomorphic to the Sierpiński curve and to the Menger curve, respectively, see [8]. A theorem by Dahmani, Guirardel, and Przytycki [6] implies that a random group at density less than $\frac{1}{2}$ in Gromov density model has a boundary homeomorphic to the Menger curve. As for nonhyperbolic CAT(0) groups, there are many examples which are known to have Sierpiński carpet boundary, but as recently as 2019, the following question was open.

Question 1. (Ruane) Does there exist a non-hyperbolic CAT(0) group G with the Menger curve boundary ?

Haulmark, Hruska, and Sathaye [19], in 2019, produced the first known examples of non-hyperbolic CAT(0) groups whose visual boundary is homeomorphic to the Menger curve. Their examples are non-right-angled Coxeter groups whose nerves are complete graphs on

vertices for $n \geq 5$. The construction in [19] depended on a slight extension of Sierpiński’s theorem on embedding 1–dimensional planar compacta into the Sierpiński carpet.

One of the main results in this dissertation is the following:

Theorem 1.1.1. *An orientable surface with a single boundary component admits (many) triangulations which are nerves of right-angled Coxeter groups with the Menger curve boundaries. Among them are many non-hyperbolic groups.*

Theorem 1.1.1 gives a new collection of positive answer to Question 1. Our examples are right-angled Coxeter groups (RACGs) whose nerves are triangulations of compact orientable surfaces with boundary, and the nerves are non-graphs. One of the key assumptions on these triangulations is “no-empty-square” condition at two special vertices, which is useful to deduce the nullity and density properties; these properties will then be exploited to prove the no local-cut point and nonplanar properties for the Menger curve.

Our proofs are based on a classical characterization of the Menger curve due to Anderson, theorems by Fischer and Świątkowski which implies the visual boundary of $\partial_\infty \Sigma_N$ (or the boundary of the right-angled Coxeter groups W_N) is Pontryagin surface, and a perturbing trick for the paths.

An outline of the proof. Now let us move on to sketching our proof. Here are several crucial steps to prove Theorem 1.1.1.

1. Denote by N a flag triangulation of an orientable surface, and W_N the corresponding right-angled Coxeter group defined as following:

$$W_N := \langle v_i \in V \mid v_i^2 = 1 \text{ for all } i, (v_i v_j)^2 = 1 \text{ if } v_i, v_j \text{ are adjacent} \rangle,$$

where V represents the vertices of N .

2. Construct the Davis CAT(0) cube complex Σ_N for the Coxeter group W_N with nerve N . Then W_N acts geometrically on Σ_N . See [10, 11] for related definitions.

3. By a theorem of Fischer [13], $\partial_\infty \Sigma_N$ is a Pontryagin surface.
4. Denote by N_0 a subcomplex obtained by removing a single vertex from N , and W_{N_0} Coxeter group with nerve N_0 , then the Davis complex for W_0 is a convex subcomplex Σ_{N_0} of Σ_N , so $\partial_\infty \Sigma_{N_0} \subseteq \partial_\infty \Sigma_N$. Note that N_0 is homeomorphic to a compact surface with a single boundary component.
5. Now we show that $\partial_\infty \Sigma_{N_0}$ can be obtained from $\partial_\infty \Sigma_N$ by removing the interiors of a pairwise disjoint, dense sequence of Pontryagin disks whose diameters converge to zero. This step requires the application of some special properties of Coxeter groups.
6. With a lot of additional work we are able to verify that $\partial_\infty \Sigma_{N_0}$ satisfies all of the conditions of a famous characterization of the Menger curve due to Anderson [2, 3]. The key steps are showing that $\partial_\infty \Sigma_{N_0}$ has no local cut points and no planar open subsets. In order to accomplish these steps (and portions of the previous step), the triangulation N from Step 1 must be chosen to satisfy some technical conditions. By adding an additional condition, we can assure that W_{N_0} is not hyperbolic.

1.2 Organization

Now we turn to state the organization of the dissertation.

In Chapter 2, we introduce CAT(0) spaces and boundary of groups, particularly some typical examples.

In Chapter 3, we discuss general properties and geometry of right-angled Coxeter groups, especially the Davis complex.

In Chapter 4, we construct a class of special triangulations. One of the key assumptions of the triangulation is “non-empty-square” property at two special vertices.

With these assumptions of the triangulations, we further investigate some special properties of the Davis complex in Chapter 5.

The “no-empty-square” property is used to deduce the nullity and density properties in Chapter 6, and the nonplanar property in Chapter 7. It is worth mentioning that an additional assumption the triangulation contains a full subcomplex Γ which is a subdivision of the barycentric subdivision of K_5 is also exploited.

In Chapter 8, we take advantage of the nullity property developed in Chapter 6, and a perturbation trick of paths to prove there is no local cut point.

Finally, we briefly prove the other properties of Menger curve, such as the visual boundary is 1-dimensional and locally connected.

Chapter 2

CAT(0) spaces and groups

2.1 CAT(0) spaces

Roughly speaking, a CAT(0) space [5] is a geodesic metric space in which all its geodesic triangles are thinner than its Euclidean triangles. More precisely, we give the definition as below.

Definition 1. (CAT(0) space) Let X be a geodesic metric space and Δ be a geodesic triangle in X . A triangle $\bar{\Delta} = \Delta(\bar{p}, \bar{q}, \bar{r})$ in Euclidean space E^n is called a **comparison triangle** for $\Delta = \Delta([p, q], [q, r], [r, p])$ if $d(\bar{p}, \bar{q}) = d(p, q)$, $d(\bar{q}, \bar{r}) = d(q, r)$ and $d(\bar{p}, \bar{r}) = d(p, r)$. See Figure 2.1. Δ is said to satisfy the **CAT(0) inequality** if for all $x, y \in \Delta$ and all comparison points $\bar{x}, \bar{y} \in \bar{\Delta}$, $d(x, y) \leq d(\bar{x}, \bar{y})$ holds. And X is called **CAT(0) space** if it is a geodesic space all of whose geodesic triangles satisfy the CAT(0) inequality.

Definition 2. The **boundary** of a proper CAT(0) space X , denoted by $\partial_\infty X$, is the set of equivalence classes of rays, where two rays are equivalent if and only if they are asymptotic. We say that two geodesic rays $\alpha, \alpha' : [0, \infty) \rightarrow X$ are **asymptotic** if there is some constant k such that $d(\alpha(t), \alpha'(t)) \leq k$ for every $t \geq 0$.

Once a base point is fixed, there is a unique representative geodesic ray from each equivalence class [5].

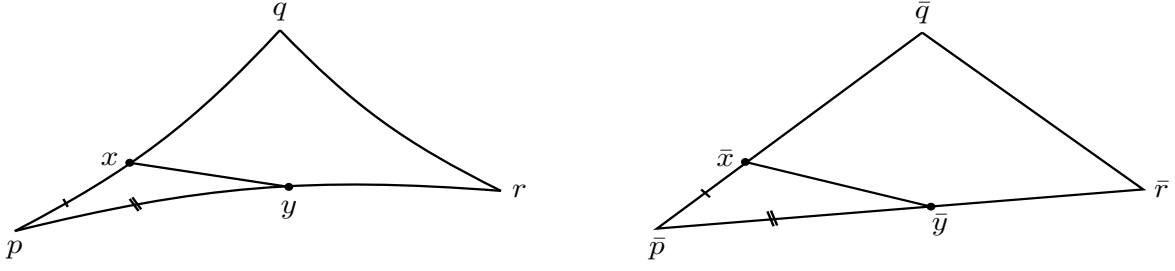


Figure 2.1: CAT(0) inequality.

We may endow $\bar{X} = X \cup \partial X$, with the cone topology, described below, which makes ∂X a closed subspace of \bar{X} and \bar{X} compact (as long as X is proper). With the topology on ∂X induced by the cone topology on \bar{X} , the boundary is often called the **visual boundary**. In what follows, the term ‘boundary’ will always mean ‘visual boundary’. Furthermore, we will slightly abuse terminology and call the cone topology restricted to $\partial_\infty X$ simply the cone topology if it is clear that we are only interested in the topology on $\partial_\infty X$.

One way in which to describe the **cone topology** on \bar{X} , denoted $\mathcal{T}(x_0)$ for $x_0 \in X$, is by giving a basis. A basic neighborhood of a point at infinity has the following form: given a geodesic ray c and positive numbers $r > 0, \epsilon > 0$, let

$$U(c, r, \epsilon) = \{x \in \bar{X} \mid d(x, c(0)) > r, d(\Pi_r(x), \Pi_r(c)) < \epsilon\},$$

where Π_r is the natural projection of \bar{X} onto $\bar{B}(c(0), r)$. Then a basis for the topology $\mathcal{T}(x_0)$, on \bar{X} consists of the set of all open balls $B(x, r) \subset X$, together with the collection of all sets of the form $U(c, r, \epsilon)$, where c is a geodesic ray with $c(0) = x_0$.

If we restrict to $\partial_\infty X$, a basis of open sets for $\partial_\infty X$ is given by all the

$$U(c, r, \epsilon) = \{\xi \in \partial_\infty X : d(\Pi_r(x), \Pi_r(c)) < \epsilon\},$$

where c is a geodesic ray, with $c(0) = x_0$ and $\epsilon, r > 0$.

Remark 1. For all $x_0, x'_0 \in X$, $\mathcal{T}(x_0)$ and $\mathcal{T}(x'_0)$ are homeomorphic, see [5] Proposition 8.8.

We need the following Lebesgue-like lemma for cone topology on $\partial_\infty X$ when (X, d) is a proper CAT(0) space.

Lemma 2.1.1. ([15])

1. For each $\gamma \in \partial_\infty X$ and $n > 0$, let

$$V(\gamma, n) = \left\{ \beta \in \partial_\infty X \mid d(\beta(n), \gamma(n)) < \frac{1}{n} \right\}.$$

Then $\left\{ V(\gamma, n) \mid \gamma \in \partial_\infty X \text{ and } n > 0 \right\}$ is a basis for the cone topology on $\partial_\infty X$.

2. For any open cover \mathcal{U} of $\partial_\infty X$, there is an $n_0 > 0$ such that each $V(\xi, n_0)$ is contained in some element of \mathcal{U} , where $\xi \in \partial_\infty X$.

We now prove some geometric properties from the CAT(0) inequality. Denote by P_δ the projection of $X \setminus B(x_0, \delta)$ onto $\partial B(x_0, \delta)$, S a subset in a CAT(0) space X , assume $\text{diam}(S) \leq A$, and S is outside the δ ball.

Lemma 2.1.2. Let κ be a constant such that $\kappa \geq 2$. If there exists a point $p_1 \in S$ with $d(x_0, p_1) \geq \kappa A$, then $\text{diam}(P_\delta(S)) \leq \frac{4\delta}{\kappa}$.

Proof. Note for any $p \in S$, we have

$$d(x_0, p) \geq d(x_0, p_1) - d(p_1, p) \geq \kappa A - A \geq \frac{\kappa A}{2}.$$

Denote $R' = d(x_0, p_1)$, $R = d(x_0, p)$, without loss of generality, we assume $R' \geq R$, see Figure 2.2, then $m := R' - R \leq d(p_1, p) \leq A$. Let q be the point on the geodesic segment $[x_0, p_1]$ with $d(x_0, q) = R$, then

$$d(p, q) \leq d(p_1, q) + d(p_1, p) \leq m + A \leq 2A.$$

Let q' and p' be the points on the geodesic line $[x_0, p_1]$ and $[x_0, p]$ with $d(x_0, q') = \delta$ and $d(x_0, p') = \delta$ respectively. Correspondingly, in the Euclidean triangle, let \tilde{q}' , \tilde{p}' be the the

points on the geodesic line $[\tilde{x}_0, \tilde{p}_1]$ and $[\tilde{x}_0, \tilde{p}]$ with $d(\tilde{x}_0, \tilde{q}') = \delta$ and $d(\tilde{x}_0, \tilde{p}') = \delta$; also denote \tilde{q} the point on the geodesic line $[\tilde{x}_0, \tilde{p}_1]$ with $d(\tilde{x}_0, \tilde{q}) = R$.

By CAT(0) inequality, we get

$$d(p', q') \leq d(\tilde{p}', \tilde{q}') = \frac{d(\tilde{p}, \tilde{q})}{R} \delta \leq \frac{2A}{\frac{1}{2}\kappa A} \delta \leq \frac{4\delta}{\kappa}.$$

□

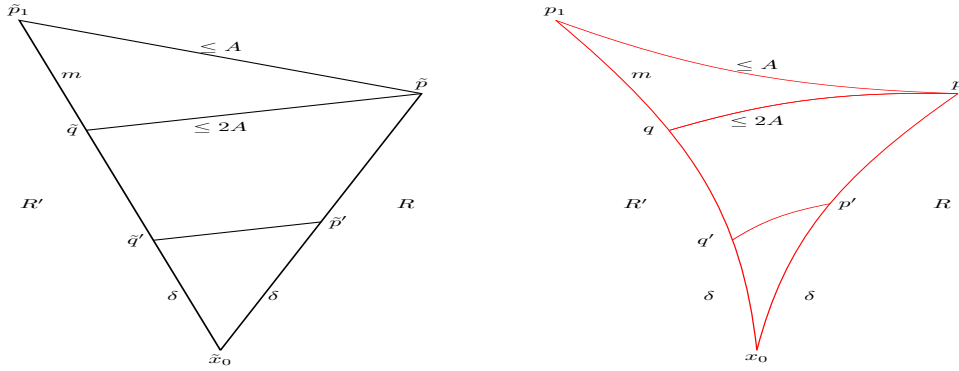


Figure 2.2: Comparison triangle.

We now give a definition of a convex set to proceed.

A subset U of X is **convex** if every $p, q \in U$ can be joined by a geodesic segment contained totally in U .

Lemma 2.1.3. *If (X, d) is CAT(0) space and Y is a closed convex subspace of X , then $(Y, d|_Y)$ is a CAT(0) space and $\partial_\infty Y$ is a subspace of $\partial_\infty X$.*

Proof. Choose a basepoint x_0 lying in Y , each geodesic ray in Y based at x_0 is also a geodesic ray in X . □

2.2 δ -hyperbolic spaces

A **δ -hyperbolic space** is a geodesic metric space with the following property: there exists a $\delta > 0$ so that the third side of any triangle lies in the δ -neighborhood of the other two. A

group G that acts geometrically (properly, cocompactly, by isometries) on a CAT(0) space [hyperbolic space] is called a **CAT(0) [hyperbolic] group**. A similar strategy to Definition 2 allows one to define ∂X for hyperbolic space X , which is called **Gromov boundary**, see [5]. ∂X is also called the **boundary of G** .

In the case when X is δ -hyperbolic CAT (0) space, the visual and Gromov boundaries are the same.

2.3 Examples of group boundaries

Here are some examples of groups and their boundaries.

Example 2.3.1.

- The boundary of \mathbb{Z} is two points, since it can act geometrically on the real line by translation; since \mathbb{R} is both CAT(0) and hyperbolic, so is \mathbb{Z} .
- Similarly, the boundary of $\mathbb{Z} \oplus \mathbb{Z}$ is a circle; $\mathbb{Z} \oplus \mathbb{Z}$ is CAT(0) but not hyperbolic.
- The boundary of 4-valent tree is the Cantor set; the free group on two generators F_2 can act on the 4-valent tree, which is both CAT(0) and hyperbolic.

Some interesting and famous fractal spaces play important roles in this dissertation because they can occur as group boundaries. Here is an informal description of a few of them.

2.3.1 Sierpiński carpet and Menger curve

The classical construction of a Sierpiński carpet (see Figure 2.3, sometimes called Sierpiński curve) is analogous to the construction of a Cantor set: start with the unit square in the plane, subdivide it into nine equal subsquares, remove the middle open square, and then repeat this procedure inductively on the remaining squares. The Menger curve can be obtained by a similar but more complicated construction, see Figure 2.4.

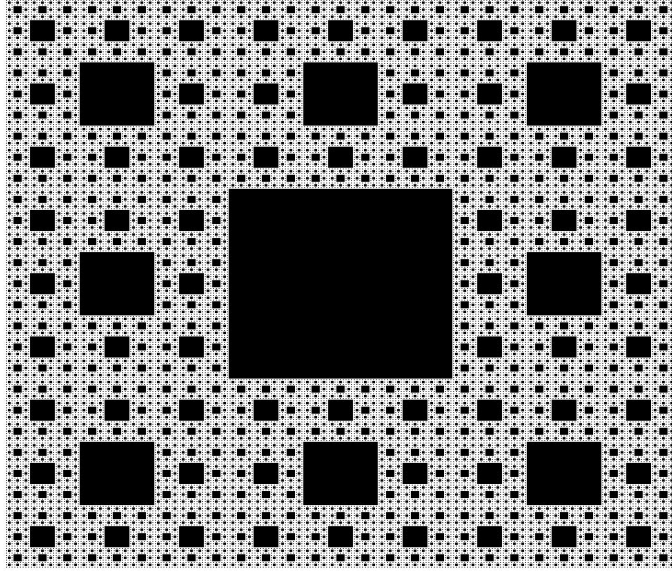


Figure 2.3: The Sierpiński carpet.

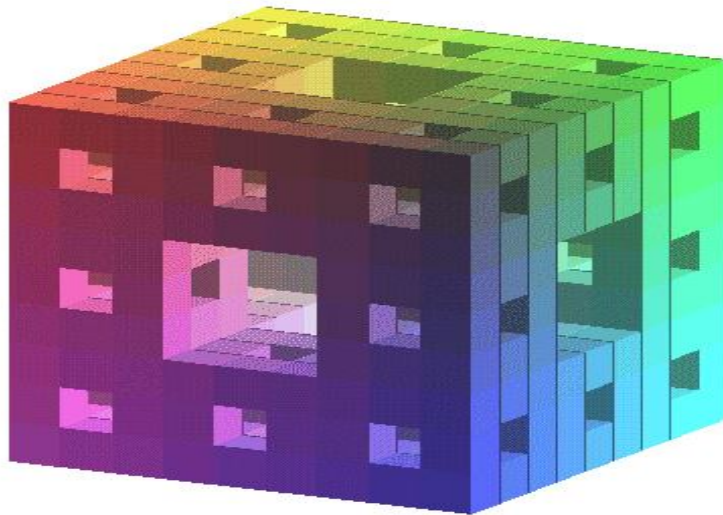


Figure 2.4: The Menger curve.

The Menger curve has the following well-known characterization:

Theorem 2.3.2. ([2, 3]) *A compact metric space M is a Menger curve provided: M is 1-dimensional, connected, locally connected, has no local-cut points, and no non-empty open subset of M is planar.*

Kapovich and Kleiner [21] investigated the hyperbolic groups with Sierpiński carpet and Menger curve boundaries. Dahmani, Guirardel, and Przytycki [22] proved that most hyperbolic groups have a boundary homeomorphic to the Menger curve. This explains the motivation of Question 1.

2.3.2 Pontryagin surface as the boundary of right-angled Coxeter group

Starting from 2-sphere \mathbb{S}^2 , remove the interiors of a disjoint dense collection of closed disks with diameters approaching zero, then glue punctured tori along the boundaries. Repeating this process infinitely many times, we get an inverse limit of an inverse sequence of connected sum of tori. We call the inverse limit the *Pontryagin surface* [9, 20, 24] denoted by \mathcal{P} , see Figure 2.5.

If we start from a Euclidean disk \mathbb{D}^2 , and then do the same process as \mathbb{S}^2 avoiding the boundary of \mathbb{D}^2 , we get the Pontryagin disk [24] denoted by $B_{\mathcal{P}}$ as an inverse limit of an inverse sequence of \mathbb{D}^2 with handles, intuitively see the part above S^1 in Figure 2.5.

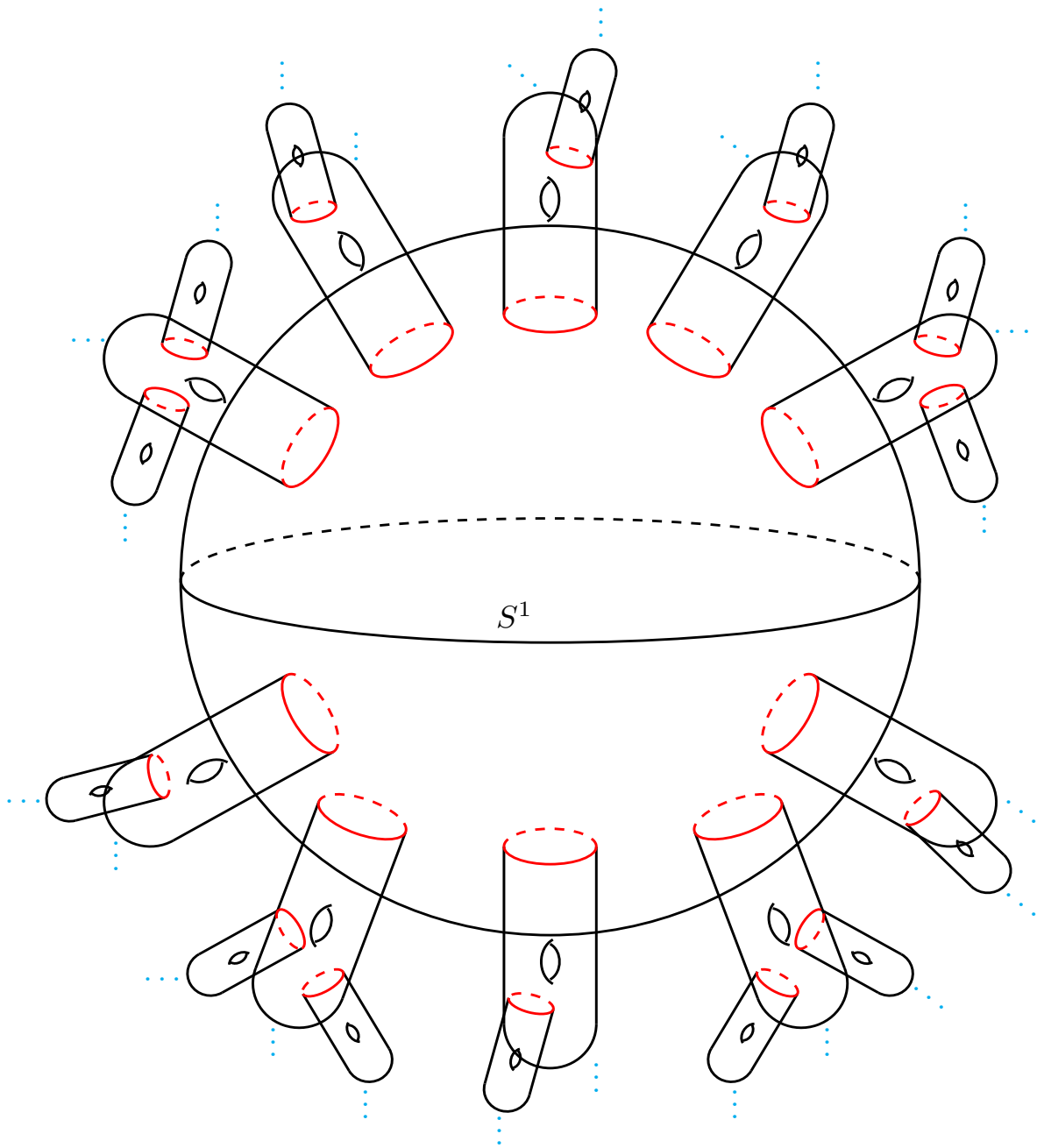


Figure 2.5: Pontryagin surface.

The Pontryagin surface \mathcal{P} has several good properties [9, 13, 24]. For instance,

- \mathcal{P} is compact, connected and 2-dimensional.
- Any separating circle S^1 divides \mathcal{P} into two components whose closures are homeomorphic to the Pontryagin disks, i.e. $\mathcal{P} \approx B_{\mathcal{P}} \cup_{S^1} B_{\mathcal{P}}$.
- For every positive integer k , \mathcal{P} is k -homogeneous, i.e., for any given two collections $\{x_1, x_2, \dots, x_k\}$ and $\{y_1, y_2, \dots, y_k\}$ of k distinct points in \mathcal{P} , there is a homeomorphism $h : \mathcal{P} \rightarrow \mathcal{P}$ such that $h(x_i) = y_i$.
- For any neighborhood U of $p \in \mathcal{P}$, there is a Pontryagin disk such that $p \in B_{\mathcal{P}} \subseteq U$.
- \mathcal{P} is locally path connected, and it has no local cut points.

A special case of Fischer's theorem [13, 29] is: if the nerve N of a right-angled Coxeter group W_N is a flag triangulation of a closed orientable surface, then the boundary of W_N is homeomorphic to the Pontryagin surface [13, 24, 34, 35], i.e. $\partial_{\infty} W_N \approx \mathcal{P}$, see more in Chapter 3.

Chapter 3

The geometry of RACGs

In Chapter 2, we introduced the Pontryagin surface as the visual boundary of right-angled Coxeter groups. In this chapter, we will explain the geometry of right-angled Coxeter groups.

In this dissertation, we restrict ourselves to surface nerve N which is a flag triangulation of a surface; N corresponds to a Coxeter group W_N , denote chamber $K = \text{cone}(N)$, gluing chambers gK (which are copies of K with $g \in W$) according to the structure of Coxeter groups, we obtain the Davis complex which Coxeter groups W act on.

3.1 Coxeter groups

Definition 3. Let V be a finite set and $m : V \times V \rightarrow \{\infty, 1, 2\}$ a function with the property that $m(u, v) = 1$ if and only if $u = v$, and $m(u, v) = m(v, u)$ for all $u, v \in V$. Then the group $W = \langle V \mid (uv)^{m(u,v)} = 1 \text{ for all } u, v \in V \rangle$ defined in terms of generators and relators is called **right angled Coxeter group**. The pair (W, V) is called a **right angled Coxeter system**.

An important feature of right angled Coxeter system is its nerve, the abstract simplicial complex

$$N = N(W, V) = \{\emptyset \neq S \subseteq V \mid \langle S \rangle \text{ is finite}\}$$

(where $\langle S \rangle$ is the subgroup of Γ generated by S), i.e., the faces correspond to vertex sets S such that $m(u, v) = 2$ for all $u, v \in S, u \neq v$. $|N|$ will denote a geometric realization of N . If N is a finite flag complex with vertex set V , then

$$W = \langle V \mid v^2 = 1 \text{ for all } v \in V \text{ and } (uv)^2 = 1 \text{ for all } \{u, v\} \in N \rangle$$

is a right angled Coxeter system whose nerve is N (see [10], Lemma 11.3). Therefore, the above describes a one-to-one correspondence between finite flag complexes N and right angled Coxeter system (W, V) .

3.2 Davis complexes

We introduce the star and the link of a vertex v denoted respectively by $St(v)$ and L_v .

Let v be a vertex of the complex \mathcal{S} , define

$$St(v) = \{\sigma \in \mathcal{S} \mid \exists \tau \in \mathcal{S}, s.t. v \in \tau \text{ and } \sigma \leq \tau\}, \quad (3.2.1)$$

and

$$L_v = \{\sigma \in St(v) \mid v \notin \sigma\}. \quad (3.2.2)$$

Let (W, V) be the right angled Coxeter system with nerve N . N' denotes the first barycentric subdivision of N . $K := cone(N')$ is called a **chamber**. Divide N' into panels

$$\left\{ P_v = |St(v, N')| \mid v \in V \right\}.$$

We give Γ the discrete topology and put

$$\Sigma_N = \Sigma(W, V) = W \times K / \sim, \quad \text{where } (g, x) \sim (h, y) \iff x = y \text{ and } g^{-1}h \in \langle v \mid x \in P_v \rangle.$$

Observe that W acts on Σ_N by left multiplication on the first coordinate. Then Σ_N is a contractible topological space on which W acts properly discontinuously: $\{g \in \Gamma \mid g(K) \cap K \neq \emptyset\}$ is finite for all compact $K \subseteq \Sigma$, see [10].

Also, Σ_N always admits a CAT(0) metric, we can interpret Σ_N as a cubical complex as follows.

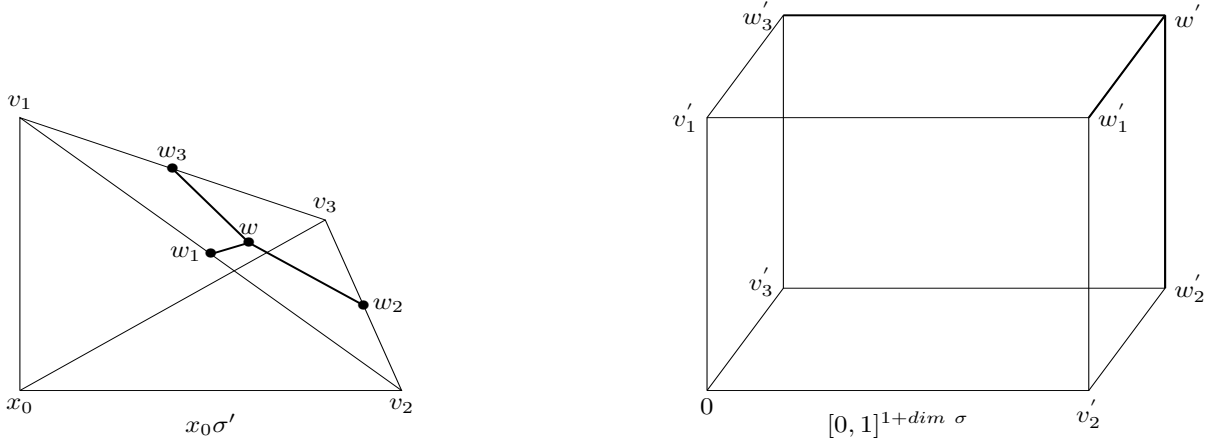


Figure 3.1: Cubification.

Cubification and piecewise Euclidean metric. Let $\sigma \in N$. Identify $|x_0\sigma'|$ with the cube $[0, 1]^{1+dim \sigma}$ as follows. The cone point x_0 corresponds to 0 and the barycenter of a face $\{v_{i_1}, v_{i_2}, \dots, v_{i_k}\}$ of σ to $e_{i_1} + e_{i_2} + \dots + e_{i_k}$, where e_{i_1}, e_{i_2}, \dots is the standard basis for Euclidean space (see Figure 3.1). The cubical complex Σ_N has a natural piecewise Euclidean CAT(0) metric [25]. This metric is given by taking the Euclidean metric of a unit cube on each of the cubes and extending it to the whole complex by taking the infima of the lengths of chains of segments such that each of these segments is contained in a single cube.

3.3 Visual boundaries of Coxeter groups

Definition 4. L is a **full subcomplex** of N if the simplices of N spanned by vertices of L are also simplices of L .

The following proposition holds, see [7].

Proposition 3.3.1. ([7]) *Let L be a full subcomplex of the nerve N of the group W_N . Then W_L is a subgroup of W_N . In particular, the homomorphism determined by the inclusion map on vertices is injective and the complex Σ_L is a convex subcomplex of Σ_N . Therefore, from Lemma 2.1.3, the boundary $\partial_\infty W_L$ is a subspace of the boundary $\partial_\infty W_N$.*

Example 3.3.2. We can now provide more context to our comments at the end of Chapter 2, N is a flag triangulation of the closed orientable surface, then $\partial_\infty W_N \approx \mathcal{P}$, where \mathcal{P} is the Pontryagin surface.

Chapter 4

Triangulation

In this chapter, we will create a class of special flag triangulations of a closed surface. The Coxeter groups corresponding to Assumption 1 given below have nice properties (see Proposition 5.3.1) which leads to the geometric retraction property of $[p, x_0]$ for $p \in g_0 W_{L_b}$ (see Proposition 6.1.2), by turn deducing the nullity and density properties. The triangulation satisfies Danielski's Theorem 3.4 in [7] which guarantees there is a nonplanar graph in the visual boundary of W_{N_1} (see Lemma 7.2.1 in Chapter 7).

4.1 Assumptions

Recall that a simplicial complex L is called a **flag complex** if each finite, non-empty set of vertices T spans a simplex in L if and only if any two elements of T span an edge (1-simplex) in L . An **empty square** in a simplicial complex is a circuit of 4 edges such that neither pair of opposite vertices is connected by an edge.

Our purpose is to construct a class of flag triangulations N of a closed surface such that the following assumptions are satisfied.

Assumption 1. N contains a pair of vertices a and b , such that neither a nor b is contained in an empty square.

Assumption 2. The edge-length distance from a to b is at least 3.

Assumption 3. $N - (a \cup b)$ contains a full subcomplex Γ which is the barycentric subdivision of one dimensional simplicial complex homeomorphic to the K_5 graph.

Remark 2. We sometimes call Assumption 1 “no-empty-square” assumption on a and b .

Remark 3. Assumption 1 implies that there does not exist a vertex in $V_{N-c} \setminus V_{L_c}$ for $c = a, b$, adjacent with two non-adjacent vertices in V_{L_c} , where V_{N-c} is the vertex set of $N - c$ and V_{L-c} is the vertex set of the link of c .

To achieve these assumptions, we provide a special construction of the triangulation.

4.2 Construction of the triangulation

Lemma 4.2.1. *There exists a (many) triangulation of a closed orientable surface of genus ≥ 1 such that the above assumptions are satisfied.*

Proof. We start with a triangulation Q of a closed orientable surface of genus ≥ 1 containing a subcomplex Γ_0 homeomorphic to K_5 , see [16, 17]. Let Q^δ be the Dranishnikov subdivision of Q (see Figure 4.1 and [7, 12]).

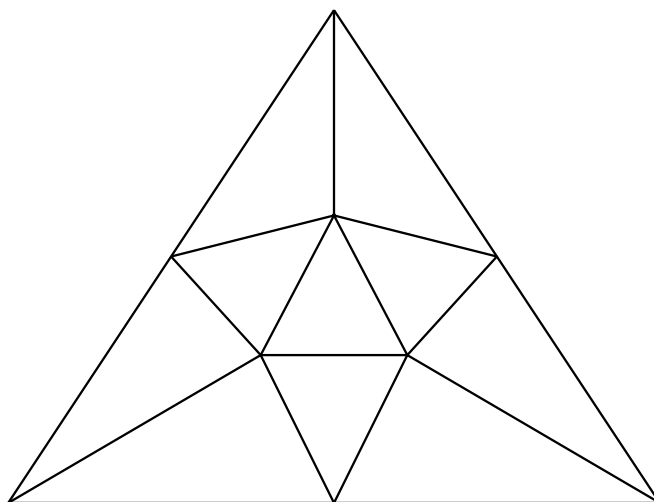


Figure 4.1: Dranishnikov subdivision of a 2-simplex.

Then, by Danieski’s Lemma 4.6 in [7], Q^δ is flag no-squares, and Γ^δ (which is the Dranishnikov subdivision of Γ ; and since each side of 2-simplex in Q is barycentrically divided in the Dranishnikov subdivision, Γ^δ is the same as the barycentric subdivision of Γ , that is Γ'_0) is a full subcomplex of Q^δ , as is every subcomplex of Γ^δ .

Next let σ_a, σ_b , and σ_c be pairwise disjoint 2-simplexes from Q , and they are disjoint from K_5 . Replace σ_c^δ with the “poison pill” triangulation of σ_c^δ (see Figure 4.2), leaving the remaining simplices of Q^δ intact. Call this new simplicial complex N . It contains a single empty square that lies in $\hat{\sigma}_c$. From each of σ_a and σ_b , choose a single interior vertex of σ_a^δ and σ_b^δ and denote these vertices by a and b , respectively. Each of their star neighborhoods E_a and E_b is full in N , as are their links (each of which is a pentagon). So too are $N - a, N - b$, and $N - (a \cup b)$. Furthermore, there are no squares in N containing a or b , and Γ'_0 is full in $N - (a \cup b)$. To fit the above notation, we may let Γ'_0 be denoted by Γ . □

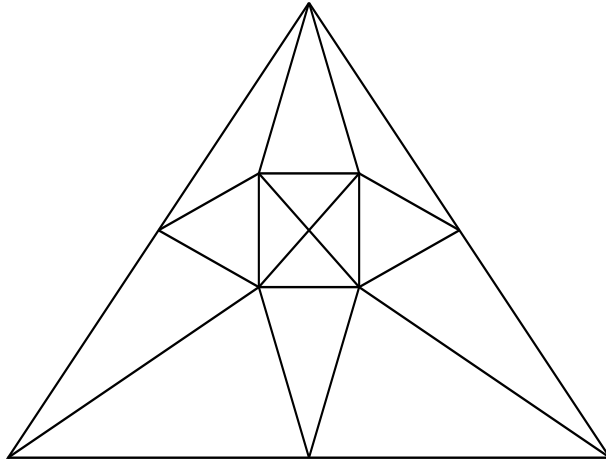


Figure 4.2: “Poison pill” subdivision.

Remark 4. In Figure 4.2, “Poison pill” contains a single empty square.

Chapter 5

More properties of Davis complex and Coxeter group

In this chapter, we investigate some new properties of Davis complex Σ_N and its visual boundary under the “no-empty-square” assumption of triangulation in Chapter 4 (see Assumption 1). More precisely, we prove the disjointness of Pontryagin disks (see Proposition 5.2.1), which will be used to prove the no local cut point property of the visual boundary $\partial_\infty \Sigma_{N_0}$ (see Chapter 8). We also develop a special property of the Coxeter groups W_N which plays an important role to prove the retraction property of geodesic segments (see Proposition 6.1.2).

5.1 Disjointness in the Davis complex

We introduce notations which will be used in this chapter. Let a represent a special vertex in the triangulation (see Chapter 4 Assumption 1).

- A word g ends in v if there exists a reduced representation of g which ends in v ; we also call this v as an ending of g . Similarly, we can define g begins in v , see [28].

- $H_a^+ := \bigcup_h \{hK : \ell(ah) < \ell(h)\}, H_a^- := \bigcup_h \{hK : \ell(ah) > \ell(h)\}.$

- $h_a := \bigcup_{g \in W_{L_a}} gP_a$, P_a is the panel with respect to a , and h_a is sometimes called a wall.
Note $h_a = H_a^+ \cap H_a^-$.

Remark 5. Note $\partial_\infty \Sigma_N = \partial_\infty H_a^+ \cup_{\partial_\infty h_a} \partial_\infty H_a^-$, and $\partial_\infty h_a = S^1$ which separates $\partial_\infty \Sigma_N$ into two homeomorphic parts, and they are Pontryagin disks, see [9].

We also need a special transversal. In the following lemma, let (W, V) be a right angled Coxeter system.

Lemma 5.1.1. ([32]) *Let $T \subseteq S$ be a subset and suppose w is a minimal length element in the left coset wW_T . Then any $w' \in wW_T$ can be written as $w' = wa'$ where $a' \in W_T$ and $\ell(w') = \ell(w) + \ell(a')$. Also wW_T has a unique minimal length element.*

Based on Lemma 5.1.1, we introduce the special transversal

- $\mathcal{J}_{N,a} := \{g', g' \text{ is the minimum length element in coset } gW_{L_a}\}$.
- $\mathcal{J}_{N,a}^+ := \{g \in \mathcal{J}_{N,a} \mid \ell(ga) > \ell(g)\}$.

Now we turn to prove some basic properties of Davis complex. Firstly, we observe a pair of inclusion relations.

Lemma 5.1.2. *Assume $g_1 \neq g_2, g_i \in \mathcal{J}_{N,a}^+, i = 1, 2$ i.e. $g_i, i = 1, 2$ does not end in a , then we have the following.*

1. *If $g_1^{-1}g_2$ ends in a , then $g_1H_a^+ \subseteq g_2H_a^+$.*
2. *If $g_1^{-1}g_2$ begins in a , then $g_2H_a^+ \subseteq g_1H_a^+$.*

Proof. Part 1: Assume $g_1^{-1}g_2 = ha$ which is a reduced representation. Let $h \in W_N$, then $g_2^{-1}g_1 = ah^{-1}$, i.e. $g_1 = g_2ah^{-1}$. Since $g_2 \in \mathcal{J}_{N,a}^+$, no letter in h^{-1} can cancel a letter of g_2 for the element in $V_N \setminus (V_{L_a} \cup a)$ do not commute with a and the elements in V_{L_a} can not reduce g_2 . Thus $g_1H_a^+ \subseteq g_2H_a^+$.

Part 2: Assume $g_1^{-1}g_2 = ah, h \in W_N$, then $g_2 = g_1ah$. Repeating the same argument as above in part 1, we can easily obtain $g_2H_a^+ \subseteq g_1H_a^+$. \square

The next lemma will be needed shortly in the proof of Lemma 5.2.4.

Lemma 5.1.3. *Assume $g_1 \neq g_2, g_i \in \mathcal{T}_{N,a}^+, i = 1, 2$ and if $g_1^{-1}g_2$ does not begin or end in a , then $g_1H_a^+ \cap g_2H_a^+ = \emptyset$.*

Proof. Suppose $g_1(w_1, x) = g_2(w_2, x) = (w, x)$ with $w_iK \subseteq H_a^+, i = 1, 2$, i.e. $g_1w_1 = g_2w_2 = w$, and $w_1 = g_1^{-1}g_2w_2$. See Figure 5.1. Note $w_2K \subseteq H_a^+$, i.e., w_2 has a reduced representation

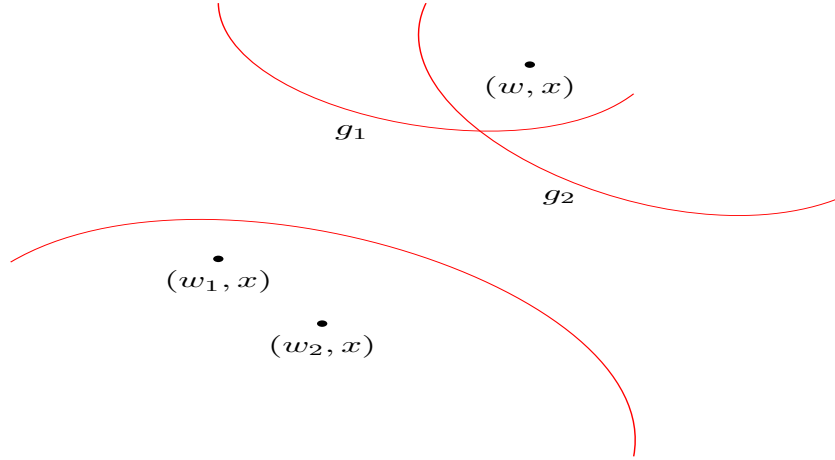


Figure 5.1: $g_1H_a^+ \cap g_2H_a^+ = \emptyset$.

ah. $g_1^{-1}g_2$ has a reduced representation which contains a generator $v \in V_N \setminus (V_{L_a} \cup a)$ since $g_i \in \mathcal{T}_{N,a}^+$ and $g_1^{-1}g_2$ does not begin or end in a , with the reduced representation ah where $h \in W_N$. So $g_1^{-1}g_2w_2$ takes the form u_1vu_2ah with u_1vu_2 as a reduced representation of $g_1^{-1}g_2$ and $v \in V_N \setminus (V_{L_a} \cup a)$, where u_1 and u_2 may be empty words. Since $g_1^{-1}g_2$ does not end in a , the beginning a in w_2 can not be cancelled, which in turn implies the v in u_1vu_2 can not be cancelled since a and v do not commute. (it can at most be cancelled by a, v in h , but that is impossible.) Further reductions are possible for the v_i 's, $v_i \in V_{L_a}$, i.e. there is a letter v_i in both u_1vu_2 and ah , and they cancel each other.

After these reductions, we may suppose $g_1^{-1}g_2w_2 = \tilde{u}_1v\tilde{u}_2a\tilde{h}$ which is reduced.

Claim 1. $ag_1^{-1}g_2w_2 = a\tilde{u}_1v\tilde{u}_2a\tilde{h}$ is a reduced representation of $g_1^{-1}g_2w_2$.

Proof of Claim 1. Since $g_1^{-1}g_2$ does not begin in a , and a does not commute with

v , the leftmost a in the above representation of $ag_1^{-1}g_2w_2$ can not be cancelled. Thus the representation $a\tilde{u}_1v\tilde{u}_2a\tilde{h}$ is reduced.

By Claim 1, $\ell(ag_1^{-1}g_2w_2) > \ell(g_1^{-1}g_2w_2)$, i.e. $w_1K \subseteq H_a^-$ where $w_1 = g_1^{-1}g_2w_2$, which implies $w_1K \subseteq H_a^+ \cap H_a^- = h_a$. Similarly, we have $w_2K \subseteq h_a$. But this implies that $g_1^{-1}g_2 \in W_{L,a}$, contradicting the fact that $g_i \in \mathcal{T}_{N,a}$. \square

5.2 Disjointness in the visual boundary

Now we are ready to prove the disjointness of Pontryagin disk, see Proposition 5.2.1 below, which will be applied to prove the no local cut point property of the visual boundary, see Chapter 8. Our aim in this section is to prove the following proposition in $\partial_\infty \Sigma_N$.

Proposition 5.2.1. *Assume $g_1 \neq g_2, g_i \in \mathcal{T}_{N,a}^+, i = 1, 2$ and $g_1^{-1}g_2$ does not begin or end in a , then $\partial_\infty(g_1H_a^+) \cap \partial_\infty(g_2H_a^+) = \emptyset$.*

Remark 6. $\partial_\infty(g_iH_a^+), i = 1, 2$ are Pontryagin disks.

Proof. Proposition 5.2.1 can be split into several lemmas as below, i.e., its proof is a combination of Lemma 5.2.4, Lemma 5.2.5, and Lemma 5.2.7. \square

Before we prove those lemmas, we make a preparation.

Lemma 5.2.2. *For any $\xi \in \partial_\infty(gH_a^+) \setminus \partial_\infty(gh_a), g \in \mathcal{T}_{N,a}^+$, the representative of ξ emanating from x_0 must intersect gh_a .*

Proof. Note gh_a separates Σ_N into two components [33]. Let γ_1 be the representative of ξ emanating from x_0 , see Figure 5.2. If $\gamma_1 \cap gh_a = \emptyset$, then γ_1 must lie in gH_a^- . Pick $y_0 \in gh_a$, let γ_2 be the representative of ξ emanating from y_0 , then γ_2 must contain a point p lying in $gH_a^+ \setminus gh_a$ since $\xi \in \partial_\infty(gH_a^+) \setminus \partial_\infty(gh_a)$ and it lies in gH_a^+ . Since gH_a^- is convex, $y_0 \in gH_a^-$, we also have a representative γ_3 of ξ emanating from y_0 . Note γ_3 must lie in gH_a^- because of the convexity of gH_a^- . But both γ_2 and γ_3 are emanating from y_0 , they should be the

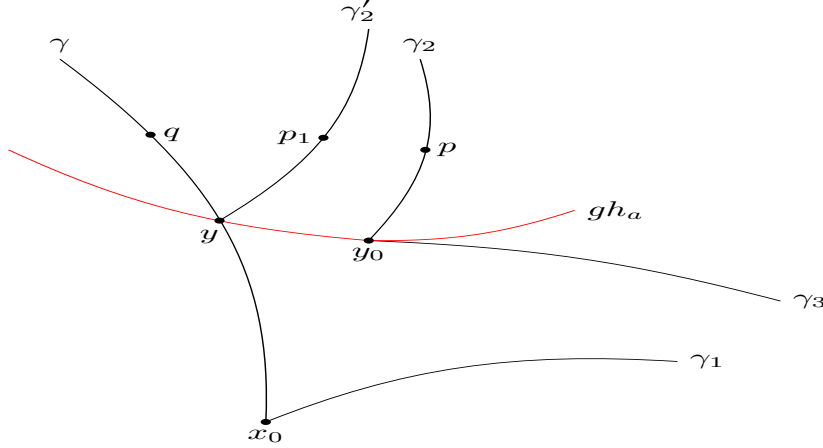


Figure 5.2: Rays intersect the wall gh_a .

same line since Σ_N is CAT(0) space. However, $gH_a^+ \setminus gh_a \ni p$ lies on γ_2 but not on γ_3 , a contradiction. So γ_1 must intersect gh_a .

□

Corollary 5.2.3. *With the same assumption as in Lemma 5.2.2, there exists a $q \in gH_a^+ \setminus gh_a$ which lies in γ and $\gamma \setminus [x_0, q] \subseteq gH_a^+ \setminus gh_a$.*

Proof. Otherwise, $\gamma \subseteq gH_a^-$. Let γ'_2 be the representative of ξ emanating from y , which must contain a point $p_1 \in gH_a^+ \setminus gh_a$ since $\xi \in \partial_\infty(gH_a^+) \setminus \partial_\infty(gh_a)$.

Denote $\gamma' := \gamma \setminus [x_0, y]$, then γ' represents ξ emanating from y , so $\gamma' = \gamma'_2$, which implies $q \in \gamma' \subseteq \gamma$.

Since gh_a is convex, $\gamma \setminus [x_0, q] \subseteq gH_a^+ \setminus gh_a$. □

Now we turn to prove the interiors of $\partial_\infty(g_i H_a^+)$ do not intersect.

Lemma 5.2.4. $\forall \xi_i \in \partial_\infty(g_i H_a^+) \setminus \partial_\infty(g_i h_a), i = 1, 2$, we have $\xi_1 \neq \xi_2$.

Proof. Let $\gamma_i, i = 1, 2$ be the representative of ξ_i emanating from x_0 , see Figure 5.3. By Lemma 5.1.3, $g_2 H_a^+ \subseteq g_1 H_a^-$. Note $x_0 \in g_1 H_a^-$, we have $\gamma_2 \subseteq g_1 H_a^-$; however, by Corollary 5.2.3, γ_1 contains a point lying in $g_1 H_a^+ \setminus g_1 h_a$, thus $\gamma_1 \neq \gamma_2$, i.e. $\xi_1 \neq \xi_2$. □

Similarly, we also have

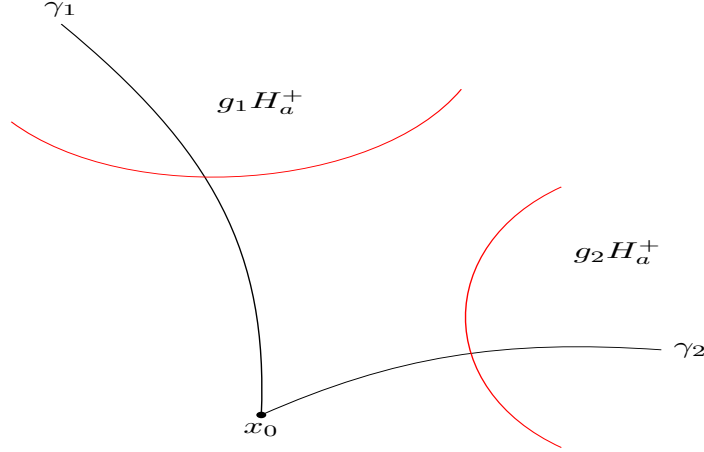


Figure 5.3: The interiors of $\partial_\infty(g_i H_a^+)$ do not intersect.

Lemma 5.2.5. *If $\xi_1 \in \partial_\infty(g_1 H_a^+) \setminus \partial_\infty(g_1 h_a)$ and $\xi_2 \in \partial_\infty(g_2 h_a)$, then we have $\xi_1 \neq \xi_2$.*

Proof. Let $\gamma_i, i = 1, 2$ be the representative of ξ_i emanating from x_0 , see Figure 5.4.

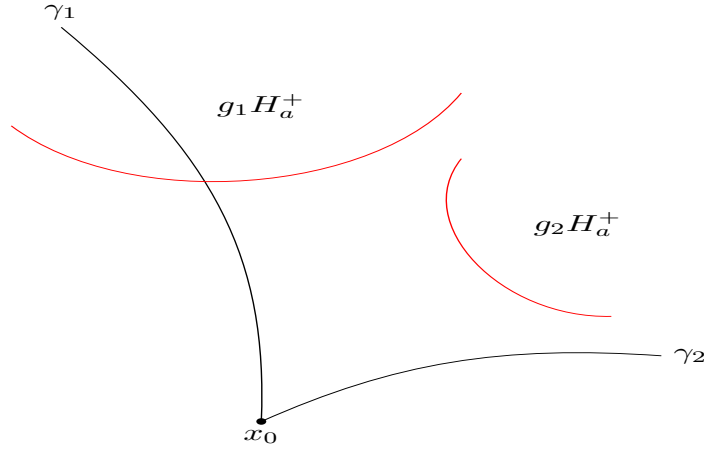


Figure 5.4: The boundary of $\partial_\infty(g_2 H_a^+)$ does not intersect with the interior of $\partial_\infty(g_1 H_a^+)$.

By Lemma 5.1.3, $g_2 H_a^+ \subseteq g_1 H_a^-$. Note $x_0 \in g_1 H_a^-$, $g_2 h_a \subseteq g_2 H_a^+$, and $g_1 H_a^-$ is convex, we have $\gamma_2 \subseteq g_1 H_a^-$; however, by Corollary 5.2.3, γ_1 contains a point lying in $g_1 H_a^+ \setminus g_1 h_a$, thus $\gamma_1 \neq \gamma_2$, i.e. $\xi_1 \neq \xi_2$. □

By the completely same process as in Lemma 5.2.5, the following corollary is immediate.

Corollary 5.2.6. *If $\xi_2 \in \partial_\infty(g_2 H_a^+) \setminus \partial_\infty(g_2 h_a)$ and $\xi_1 \in \partial_\infty(g_1 h_a)$, then we have $\xi_1 \neq \xi_2$.*

Finally, we prove the boundaries of $\partial_\infty(g_i h_a)$ do not intersect.

Lemma 5.2.7. *Assume $g_1 \neq g_2, g_i \in \mathcal{T}_{N,a}^+, i = 1, 2$ and $g_1^{-1}g_2$ does not begin or end in a , then $\partial_\infty(g_1 h_a) \cap \partial_\infty(g_2 h_a) = \emptyset$.*

Proof. Recall L_a is the link of a ; W_{L_a} is the group generated by the vertices of L_a . $\forall \xi_i \in \partial_\infty(g_i H_a^+), i = 1, 2$, there exists a unique geodesic line γ_i emanating from $g_i x_0$, which lies in $g_i W_{L_a} K$, choose $\gamma_i(j)$ such that $\gamma_i(j) \in g_i h_{ij} K, h_{ij} \in W_{L_a}$, and $\ell(h_{ij}) \rightarrow \infty$ as $j \rightarrow \infty$.

We aim at proving $\xi_1 \neq \xi_2$, i.e. to prove the Hausdorff distance $d_{\mathbb{H}}(r_1, r_2)$ ([5] page 70) is unbounded, it is sufficient to prove

$$\ell((g_1 h_{1j})^{-1} g_2 h_{2j}) \rightarrow \infty, \quad \text{as } j \rightarrow \infty. \quad (5.2.1)$$

Note that $(g_1 h_{1j})^{-1} g_2 h_{2j} = h_{1j}^{-1} g_1^{-1} g_2 h_{2j}$, since $g_1 \neq g_2, g_1^{-1} g_2 \notin W_{L_a}$, which implies every reduced representation of $g_1^{-1} g_2$ contains some element in $V_{N_0} \setminus (V_{L_a} \cup a)$, say v_3 . By Assumption 1 in Chapter 4, v_3 is adjacent to at most two vertices from L_a . Moreover, if there are two such vertices, then they are adjacent, say v_1 and v_2 .

Suppose $h_{1j}^{-1} g_1^{-1} g_2 h_{2j}$ takes the form of $h_{1j}^{-1} w_1 v_3 w_2 h_{2j}$ with $w_1 v_3 w_2$ as a reduced representation of $g_1^{-1} g_2$ (w_1 and w_2 may be the empty word).

After the cancellation between h_{1j}^{-1} and w_1, w_2 and h_{2j} , we can write $h_{1j}^{-1} g_1^{-1} g_2 h_{2j}$ as $\tilde{h}_{1j}^{-1} \tilde{w}_1 v_3 \tilde{w}_2 \tilde{h}_{2j}$ with $\tilde{h}_{1j}^{-1} \tilde{w}_1$ and $\tilde{w}_2 \tilde{h}_{2j}$ are reduced.

Further reduction are possible only if there is a reduced representation for $\tilde{w}_2 \tilde{h}_{2j}$ beginning with v_1 or v_2 , which can lead to at most two additional cancellations since $\tilde{w}_2 \tilde{h}_{2j}$ is reduced.

Note

$$\ell(\tilde{h}_{1j}^{-1} \tilde{w}_1) \geq \ell(h_{1j}) - \ell(w_1) \quad \text{and} \quad \ell(\tilde{w}_2 \tilde{h}_{2j}) \geq \ell(h_{2j}) - \ell(w_2),$$

we have

$$\begin{aligned} \ell(h_{1j}^{-1} g_1^{-1} g_2 h_{2j}) &= \ell(\tilde{h}_{1j}^{-1} \tilde{w}_1 v_3 \tilde{w}_2 \tilde{h}_{2j}) \\ &\geq \ell(\tilde{h}_{1j}^{-1} \tilde{w}_1) + \ell(\tilde{w}_2 \tilde{h}_{2j}) + 1 - 2 \cdot 2 \\ &\geq \ell(h_{1j}^{-1}) - \ell(w_1) + \ell(h_{2j}) - \ell(w_2) - 3 \rightarrow \infty, \end{aligned} \quad (5.2.2)$$

as $j \rightarrow \infty$ since $\ell(w_i)$ is finite (only depends on g_1 and g_2). □

5.3 Special property of Coxeter groups

In this section, we assume Assumption 1 holds for vertex a defined in Chapter 4. The following proposition will be used to prove a nice geodesic retraction property, see Proposition 6.1.2 in Chapter 6.

Let us recall $In(g) := \{v \in V_N \mid \ell(gv) < \ell(g)\}$.

Proposition 5.3.1. *Suppose $g \in \mathcal{T}_{N,a}^+$, $h \in W_{L_a}$, gh is reduced, i.e., $\ell(gh) = \ell(g) + \ell(h)$, and $\ell(h) \geq 3$, then $In(gh) \subseteq V_{L_a}$.*

Remark 7. Since we impose the same assumption on b as on a , this proposition also holds for b .

Proof. Obviously, $a \notin In(gh)$ because $\ell(ga) > \ell(g)$. Since $g \in \mathcal{T}_{N,a}^+$, g ends in $w \in V_{N-a} \setminus V_{L_a}$, and h can be expressed by the vertices only from L_a , gh is reduced.

Case 1: h can be represented by a reduced word involving only two generators from V_{L_a} . In this case, h takes the form $v_i v_j v_i v_j \cdots$, where v_i and v_j do not commute, and $v_i \neq v_j$.

Claim 2. $w \in V_{N-a} \setminus V_{L_a} \Rightarrow w \notin In(gh)$.

Proof of Claim 2. Otherwise, if $\ell(ghw) < \ell(gh)$, then w must commute with v_i and v_j , a contradiction to Assumption 1.

Case 2: h can be represented by a reduced word involving more than two generators from V_{L_a} .

In this case $h = v_1 v_2 v_3 \cdots v_l$, where $\{v_1, \cdots, v_l\}$ contains three distinct elements, say v_i, v_j , and v_k .

Claim 3. $w_1 \in V_{N-a} \setminus V_{L_a} \Rightarrow w_1 \notin In(gh)$.

Proof of Claim 3. Otherwise, if $\ell(ghw_1) < \ell(gh)$, this implies w_1 can commute with all of v'_m s, but by Assumption 1, v_i must commute with each other, $\{w_1, v_i, v_j, v_k\}$ would constitute a 3-simplex in N , contradicting the fact that the triangulation is 2-dimensional.

If h contains more than two different vertices, say $h = v_1v_2v_3 \cdots$, v_1, v_2 and v_3 are different, then $In(gh)$ does not contain any vertex in V_{N-a} ; otherwise if there exists $w_1 \in In(gh)$, i.e. $\ell(ghw_1) < \ell(gh)$, then w_1 can cancel some w_1 in g (h does not contain any vertex in V_{N-a}), this implies w_1 can commute with all of $v_i, i = 1, 2, 3$, but by Assumption 1, $v_i, i = 1, 2, 3$ must be adjacent to each other, i.e. they commute pairwise; however, (w_1, v_1, v_2, v_3) would constitute a 3-simplex, which contradicts the fact that the nerve is 2-dimensional. \square

Remark 8. Since we impose the same assumption on b as on a , all of the properties in this chapter holds for b as well.

Chapter 6

Nullity and density

In this chapter, we aim at deriving nice nullity and density properties, i.e., $\{\partial_\infty(\hat{g}H_a^+)\}_{\hat{g} \in \mathcal{F}_{N_0, a}}$ is null in $\partial_\infty \Sigma_N$ and $\{\partial_\infty(\hat{g}H_b^+) \cap \partial_\infty \Sigma_{N_0}\}_{\hat{g} \in \mathcal{F}_{N_0, b}^+}$ is dense in $\partial_\infty \Sigma_{N_0}$. These properties play a crucial role in proving the nonplanar and no local cut point properties of $\partial_\infty \Sigma_{N_0}$. In particular, the nullity property is derived from a nice retraction property of geodesic segment, which is based on the fact $[p, x_0]$ intersects the mirrors gP_v of gK with some $v \in \text{In}(g)$, and “no-empty-square” assumption on special vertices (see Assumption 1 in Chapter 4). The density property can be deduced similarly.

6.1 Properties of geodesic segments

In this subsection, we need the following notations.

- $h_{v_i} := \bigcup_{g \in W_{L_{v_i}}} gP_{v_i}$, where L_{v_i} is the link of v_i , h_{v_i} is the fixed set of the reflection v_i viewed as an element of W_N , it is sometimes called a wall. The wall separates Σ_N into two components, denote the closure of the component without the fundamental chamber by $H_{v_i}^+$ and the component containing the fundamental chamber by $H_{v_i}^-$.
- $\text{In}(g) := \{v \in V_N : \ell(gv) < \ell(g)\}$.

First of all, we would like to prove a special geometric property of geodesic segments

which is useful to establish the nullity and density properties. Denote by $[p, x_0]$ the geodesic segment (with CAT(0) path length metric) starting at p and ending at x_0 (unique path).

Proposition 6.1.1. *For any point $p \in gK$, $[p, x_0]$ must intersect $\bigcup_{v \in In(g)} gP_v$.*

Proof. We split our proof into three cases.

Case 1. $p \in gP_{v_i}$ for some $v_i \in In(g)$, we are done.

Case 2. $p \in gP_{v_{k_j}} \setminus \bigcup_{v_i \in In(g)} gP_{v_i}, v_{k_j} \in Out(g), 1 \leq j \leq n$.

In this case, p can only lie in the chambers $\tilde{g}K$ with $\tilde{g} \in gW_V$, where W_V is generated by $V = \{v_{k_1}, \dots, v_{k_n}\}$.

$\forall y \in \tilde{g}K \setminus gK, \tilde{g} \in g(W_V \setminus \{e\})$, there exists a $v_{k_i}, 1 \leq i \leq n$, such that y lies in the side of the wall $gh_{v_{k_i}}$ without the fundamental chamber. And $[p, x_0]$ is a geodesic segment which can not across $gh_{v_{k_i}}$ twice (see [14], since $gh_{v_{k_i}}$ is convex and Σ_N is CAT (0) space). Thus

$$[p, x_0] \cap (\tilde{g}K \setminus gK) = \emptyset. \quad (6.1.1)$$

Let $[p, x_0] = \bigcup_{i=1} S_i$, each S_i is a maximal subsegment of $[p, x_0]$ lies in a single cube of a chamber.

Now we have $S_1 \cap (\tilde{g}K \setminus gK) = \emptyset$ by (6.1.1). But S_1 should lie in some $\hat{g}K$ with $\hat{g}K \in gW_v$, so $S_1 \subseteq gK$.

Denote $j := \min\{i : S_i \setminus gK \neq \emptyset \text{ but } S_{i-1} \setminus gK = \emptyset\}$, j exists since each cube can only contain one segment and each chamber contains finitely many cubes.

Let $Q := S_j \cap S_{j-1}$, then $Q \in gP_{v_i}$ for some $V_i \in In(g)$.

Case 3. $p \in g\mathring{K}$, i.e., p lies in the interior of gK . Note gN separates Σ_N , so $\forall p \in gK, [p, x_0] \cap gN \neq \emptyset$, then Case 3 is reduced to Case 1 and Case 2.

Thus we complete the proof of this proposition. □

Now we are devoted to proving the following property: $\forall p \in gK, g \in \hat{g}W_{L_b}, \hat{g} \in \mathcal{J}_{N_0, b}^+, p$ retracts to some point around $\hat{g}K$, see Proposition 6.1.2.

Let

$$G_{1,\hat{g}} = \{g \in \hat{g}W_{L_b} \mid \ell(\hat{g}^{-1}g) \leq 2\}, \quad G_{2,\hat{g}} = \hat{g}W_{L_b} \setminus G_{1,\hat{g}},$$

where W_{L_b} is subgroup generated by V_{L_b} , \hat{g} is the minimum length element (word metric) in a coset $\hat{g}W_{L_b}$ for W_{N_0} .

Proposition 6.1.2. *Assume Assumption 1 in Chapter 4 holds, then $\forall p \in gK, g \in G_{2,\hat{g}}$, we have $[p, x_0] \cap G_{1,\hat{g}}K \neq \emptyset$.*

Proof. Case 1: For $g \in G_2$ with $\ell(\hat{g}^{-1}g) \geq 5$.

Note $gP_{v_i} = (gv_i)P_{v_i}$, from Proposition 6.1.1, $\forall p \in gK, [p, x_0] \cap (gv_i)K \neq \emptyset$, for some $v_i \in \text{In}(g) \subseteq V_{L_b}$ with $gv_i \in G_2$ (by Proposition 5.3.1 and Remark 8).

Note $\ell(gv_i\hat{g}^{-1}) \geq 4$, by Proposition 5.3.1, $\text{In}(gv_i) \subseteq V_{L_b}$; then for some $v_j \in \text{In}(gv_i)$, $[p, x_0] \cap (gv_iv_j)K \neq \emptyset$ (by Proposition 6.1.1) with $gv_iv_j \in G_2$.

Since $\ell(\hat{g}^{-1}gv_iv_j) < \ell(\hat{g}^{-1}gv_i) < \ell(\hat{g}^{-1}g)$, i.e., $\ell(\hat{g}^{-1}g)$ with $g \in G_2$ is decreasing, inductively applying Proposition 6.1.1 and Proposition 5.3.1 on the length $\ell(\hat{g}^{-1}g)$ completes the proof.

Case 2: For $g \in G_2$ with $\ell(\hat{g}^{-1}g) \leq 4$.

Repeating the above process in two steps is enough. □

Remark 9. The propositions above hold for a vertex as well since we impose the same assumptions as b vertex.

6.2 Nullity property

With the above preparation, we are ready to prove $\{\partial_\infty(\hat{g}H_a^+)\}_{\hat{g} \in \mathcal{J}_{N_0,a}}$ is null in $\partial_\infty \Sigma_N$ and $\{\partial_\infty(\hat{g}H_b^+) \cap \partial_\infty \Sigma_{N_0}\}_{\hat{g} \in \mathcal{J}_{N_0,b}^+}$ is dense in $\partial_\infty \Sigma_{N_0}$, which will be used to prove the nonplanar property in Chapter 7.

Before we prove the nullity property above, we introduce notations and definitions needed in this section.

- $\forall \xi \in \partial_\infty \Sigma_N$, let γ_ξ represent the ray for ξ based at x_0 , or simply γ if no confusion arises.
- $V(\gamma, n) = \left\{ \beta \in \partial_\infty X \mid d(\beta(n), \gamma(n)) < \frac{1}{n} \right\}$.
- $\Pi_\delta(\xi) : \text{the projection of } \xi \text{ onto } \partial B(x_0, \delta), \quad \Pi_\delta : \partial_\infty \Sigma_N \longrightarrow \partial B(x_0, \delta)$.
- $U_{\Pi_\delta(\xi)} : \text{a neighborhood of } \Pi_\delta(\xi) \text{ in } \partial B(x_0, \delta)$.
- $W_{L_b}K \cap (bW_{L_b})K = hb; \quad (gW_{L_b})K \cap (gbW_{L_b})K = ghb$.
- Denote $\mathcal{T}_{N_0, b} := \{g' : g' \text{ is the unique minimum length element in coset } g'W_{L_b} \text{ of } W_{N_0}\}$;
 $\mathcal{T}_{N_0, b}^+ := \{g \in \mathcal{T}_{N_0, b} : \ell(gb) > \ell(g)\}$.

Fact 1. Let

$$\tilde{G}_{1, \hat{g}} = \{g \in W_{N_0} \mid \ell(\hat{g}^{-1}g) \leq 10\}, \quad \tilde{G}_{1, \hat{g}}K = \bigcup_{g \in \tilde{G}_{1, \hat{g}}} gK,$$

then there exists an $A > 0$, which is independent of \hat{g} , such that $\text{diam}(\tilde{G}_{1, \hat{g}}K) \leq A$.

Lemma 6.2.1. *Let $g_1 \in \mathcal{T}_{N_0, b}, t \in W_{L_b}$, and g_1t is reduced, $s \in V_{N_0}$ and does not commute with any generator of W_{L_b} , then $g_1ts \in \mathcal{T}_{N_0, b}^+$, and g_1ts is reduced.*

Proof. Note g_1t is reduced, by assumption, s can not cancel any s (if there is any) in g_1t , so g_1ts is reduced. Also, b does not commute with s , thus $g_1ts \in \mathcal{T}_{N_0, b}^+$. \square

Proposition 6.2.2. $\forall n > 0, \xi \in \partial_\infty \Sigma_{N_0}$ and $V(\xi, n) \subseteq \partial_\infty \Sigma_N$, there exists a $\hat{g} \in \mathcal{T}_{N_0, b}^+$ such that $\partial_\infty(\hat{g}H_b^+) \subseteq V(\xi, n)$.

Proof. Note $\forall x \in \Sigma_{N_0}, \exists g \in \mathcal{T}_{N_0, b}$ such that $x \in (gW_{L_b})K$, we have $\forall \gamma \in \partial_\infty \Sigma_{N_0}, \forall R > 0, \exists h \in W_{N_0}$, such that $\gamma(R) \in hK$ and $\exists g_1 \in \mathcal{T}_{N_0, b}$, such that $h \in g_1W_{L_b}$, so $\gamma(R) \in (g_1W_{L_b})K$. Applying this to ξ , let $\xi(R) \in hK$ for some $h \in W_{N_0}$, we can rewrite $h = g_1t, t \in W_{L_b}, g_1 \in \mathcal{T}_{N_0, b}$ (If t is trivial, then $h = g_1$). Take $\hat{g} = g_1ts$, where $s \in V_{N_0}$ does not commute with any vertex in L_b , see Figure 6.1, by Lemma 6.2.1, $\hat{g} \in \mathcal{T}_{N_0, b}^+$. We can choose R sufficiently large such that $\text{diam}(\Pi_n(\tilde{G}_{1, \hat{g}}K)) < \frac{1}{2n}$ by Lemma 2.1.2. Note $\xi(n) \in \Pi_n(\tilde{G}_{1, \hat{g}}K)$, we have

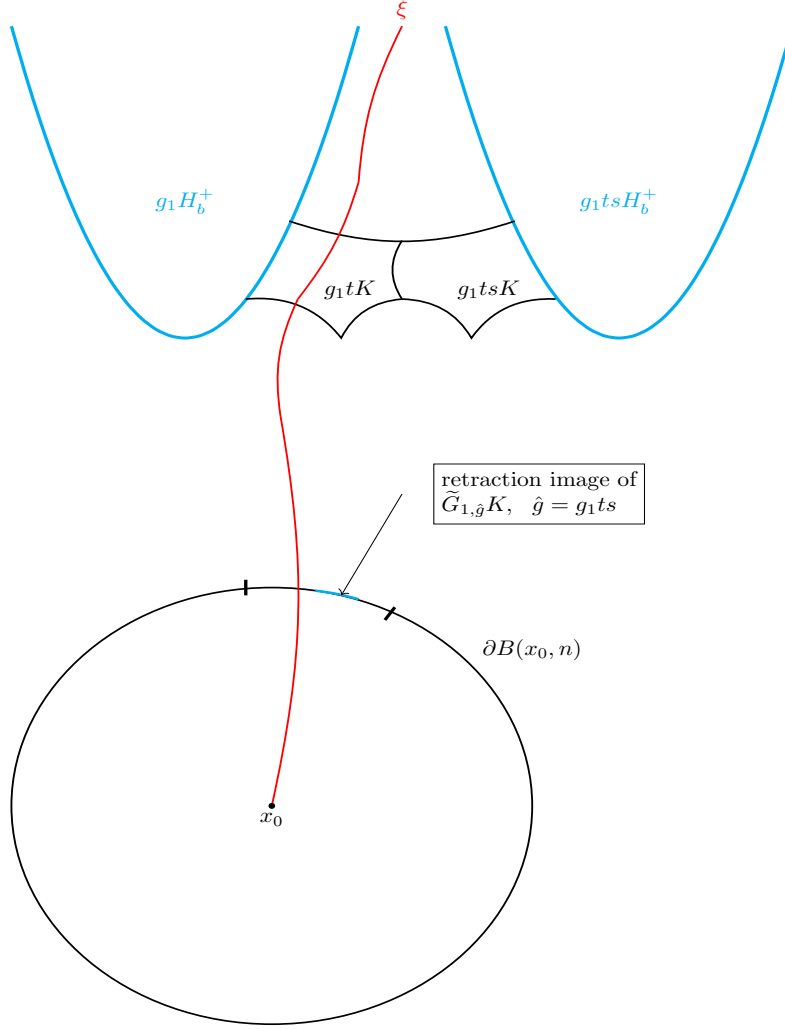


Figure 6.1: $\tilde{G}_{1,\hat{g}}K$ retracts onto $\partial B(x_0, n)$ and $\Pi_n(\tilde{G}_{1,\hat{g}}K) \subseteq B_{\frac{1}{n}}(\xi(n))$.

$\Pi_n(\tilde{G}_{1,\hat{g}}K) \subseteq B_{\frac{1}{n}}(\xi(n))$. Since $G_{1,\hat{g}}K \subseteq \tilde{G}_{1,\hat{g}}K$, we have $\Pi_n(G_{1,\hat{g}}K) \subseteq \Pi_n(\tilde{G}_{1,\hat{g}}K)$. Note $\forall \eta \in \partial_\infty(\hat{g}H_b^+)$, $\gamma_\eta \cap G_{1,\hat{g}}K \neq \emptyset$, we deduce that each ray based at x_0 that intersects $G_{1,\hat{g}}K$ is contained in $V(\xi, n)$, thus completes the proof. \square

Now the following corollary is immediate since $V(\xi, n)$ is a basis of $\partial_\infty \Sigma_N$.

Corollary 6.2.3. $\forall \xi \in \partial_\infty \Sigma_{N_0}$, let U be a neighborhood of ξ in $\partial_\infty \Sigma_N$, then there exists a $\hat{g} \in \mathcal{T}_{N_0, b}^+$ such that $\partial_\infty(\hat{g}H_b^+) \subseteq U$.

Then we can further deduce the density property.

Corollary 6.2.4. *(Density)* $\{\partial_\infty(\hat{g}H_b^+) \cap \partial_\infty\Sigma_{N_0}\}_{\hat{g} \in \mathcal{T}_{N_0,b}}$ is dense in $\partial_\infty\Sigma_{N_0}$, i.e.,
 $\forall \hat{U} \subseteq \partial_\infty\Sigma_{N_0}, \exists \hat{g}$ s.t. $\partial_\infty(\hat{g}H_b^+) \cap \partial_\infty\Sigma_{N_0} \subseteq \hat{U}$.

Proof. $\forall \hat{U} \subseteq \partial_\infty\Sigma_{N_0}, \exists U \subseteq \partial_\infty\Sigma_N$ s.t. $\hat{U} = U \cap \partial_\infty\Sigma_{N_0}$ by the subspace topology.

By Corollary 6.2.3, $\exists \hat{g} \in \mathcal{T}_{N_0,b}^+$ s.t. $\partial_\infty(\hat{g}H_b^+) \cap \partial_\infty\Sigma_{N_0} \subseteq U \cap \partial_\infty\Sigma_{N_0} = \hat{U}$. \square

The above argument can be applied to prove the nullity property. Let us recall a basic fact about the nullity.

Recall that a family of subsets \mathcal{Z} is **null** in a metric space X if for every $\epsilon > 0$ the set $\{Z \in \mathcal{Z} \mid \text{diam } Z > \epsilon\}$ is finite.

Lemma 6.2.5. *A collection $\{A_n\}_{n=1}^\infty$ of subsets of a compact metric space X is a null sequence if for any $\epsilon > 0$ and open cover $\mathcal{U}_\epsilon = \{B(x, \frac{\epsilon}{2})\}$ of X , $\exists M(\epsilon) > 0$ s.t. each A_n is contained in some \mathcal{U}_ϵ if $n > M$.*

Proof. This follows immediately from the definition of nullity. \square

Proposition 6.2.6. $\{\partial_\infty(gH_a^+)\}_{g \in \mathcal{T}_{N_0,a}}$ is null.

Proof. By Lemma 2.1.1, for \mathcal{U}_ϵ as in Lemma 6.2.5, there exists an $n_0(\epsilon)$ such that $V(\xi, n_0)$ is contained in some element of \mathcal{U}_ϵ for any $\xi \in \partial_\infty\Sigma_N$. Note that we impose the same assumption on a as on b , by the same process as in Proposition 6.2.2, we have, for $g \in \mathcal{T}_{N_0,a}$ with $d(g, 1)$ sufficiently large such that $\forall \xi \in \partial_\infty(gH_a^+), \partial_\infty(gH_a^+) \subseteq V(\xi, n_0)$, which completes the proof. \square

Chapter 7

Locally nonplanar property

With the density property obtained in last chapter, we are ready to prove the locally nonplanar property. More precisely, we are going to prove the statement: for any $\xi \in \partial_\infty \Sigma_{N_0}$, and any neighborhood \widehat{U} of ξ , there exists a \widetilde{U}_j and a nonplanar graph G_{non} such that $G_{non} \subseteq \partial_\infty \widetilde{U}_j \cap \partial_\infty \Sigma_{N_0} \subseteq \widehat{U}$. Firstly, by the triangulation, especially Assumption 3 in Chapter 4, and Danielski's Theorem 3.4 in [7], we can find a nonplanar graph $G_{non} \subseteq \partial_\infty \Sigma_{N_1}$. Secondly, since $\partial_\infty \Sigma_{N_1} \subseteq \partial_\infty \Sigma_N$, and there are copies of G_{non} in $\partial_\infty \widetilde{U}_j$ for any j ; thanks to the density property, we can derive that there exists a G_{non} in any open set $\widehat{U} \subseteq \partial_\infty \Sigma_{N_0}$, i.e., locally nonplanar property.

7.1 Notations

We need the following notations.

- $N_0 := N - a, N_1 := N - (a \cup b)$.
- $\mathcal{T}_{N_0,b}$: a special transversal of W_{N_0} for W_{L_b} , i.e.
 $\mathcal{T}_{N_0,b} := \{g' : g' \text{ is the unique minimum length element in coset } gW_{L_b}\}$.
 $\mathcal{T}_{N_0,b}^+ := \{g \in \mathcal{T}_a \mid \ell(ga) > \ell(g)\}$.
- gH_a^+ : the translation of H_a^+ by $g \in \mathcal{T}_{N_0,a}$, where

$\mathcal{T}_{N_0,a} := \{g' : g' \text{ is the unique minimum length element in a coset } gW_{L_a}\}.$

- $\mathcal{U}_i := g_i H_a^+, g_i \in \mathcal{T}_{N_0,a}; \tilde{\mathcal{U}}_j := g_j H_b^+, g_j \in \mathcal{T}_{N_0,b}^+$ (see Figure 7.1, Figure 7.2, Figure 7.3, and Figure 7.4).

7.2 Proof of the locally nonplanar property

We need the following lemma.

Lemma 7.2.1. ([7, 19]) *The visual boundary of the Davis complex for the barycentric subdivision of one dimensional simplicial complex homeomorphic to the K_5 graph contains a nonplanar graph.*

Remark 10. This lemma is a simple application of Theorem 3.4 in [7].

To show the locally nonplanar property, it suffices to prove the following proposition.

Proposition 7.2.2. $\forall \xi \in \partial_\infty \Sigma_{N_0}$, and any neighborhood \hat{U} of ξ , $\hat{U} \subseteq \partial_\infty \Sigma_{N_0}$, there exists a nonplanar graph $G_{non} \subseteq \hat{U}$.

Proof. By Lemma 7.2.1 and Assumption 3 in Chapter 4, i.e., the subdivision of K_5 is full, there exists a nonplanar graph $G_{non} \subseteq \partial_\infty \Sigma_{N_1}$ (see Figure 7.3, the green star in the boundary represents G_{non}); since each $\tilde{\mathcal{U}}_j$ contains a copy of Σ_{N_1} by the following Lemma 7.2.3, (see Figure 7.2 and Figure 7.4, the yellow part in $\tilde{\mathcal{U}}_j$ is Σ_{N_1}), we also have a copy of G_{non} in $\partial_\infty \tilde{\mathcal{U}}_j$ for each j and $G_{non} \subseteq \partial_\infty \Sigma_{N_0}$. By the subspace topology, there exists a U such that $\hat{U} = U \cap \partial_\infty \Sigma_{N_0}$. By Corollary 6.2.4, it holds $(\partial_\infty \tilde{\mathcal{U}}_j) \cap \partial_\infty \Sigma_{N_0} \subseteq \hat{U}$. Thus $G_{non} \subseteq \hat{U}$. \square

The following lemma indicates the copy of Σ_{N_1} in $\tilde{\mathcal{U}}_j$ for each j would miss any \mathcal{U}_i .

Lemma 7.2.3. $\forall h \in W_{N_1}, g_1 \in \mathcal{T}_{N_0,b}^+, g \in \mathcal{T}_{N_0,a}, (g_1 b g_1^{-1})h \subseteq gH_a^-.$

Proof. Note h, g, g_1 do not contain the element a , however, any chamber lying in gH_a^+ must take a (reduced) form gaw , where $g \in \mathcal{T}_{N_0,a}$ and $w \in W_N$, thus $(g_1 b g_1^{-1})h \subseteq gH_a^-$. \square

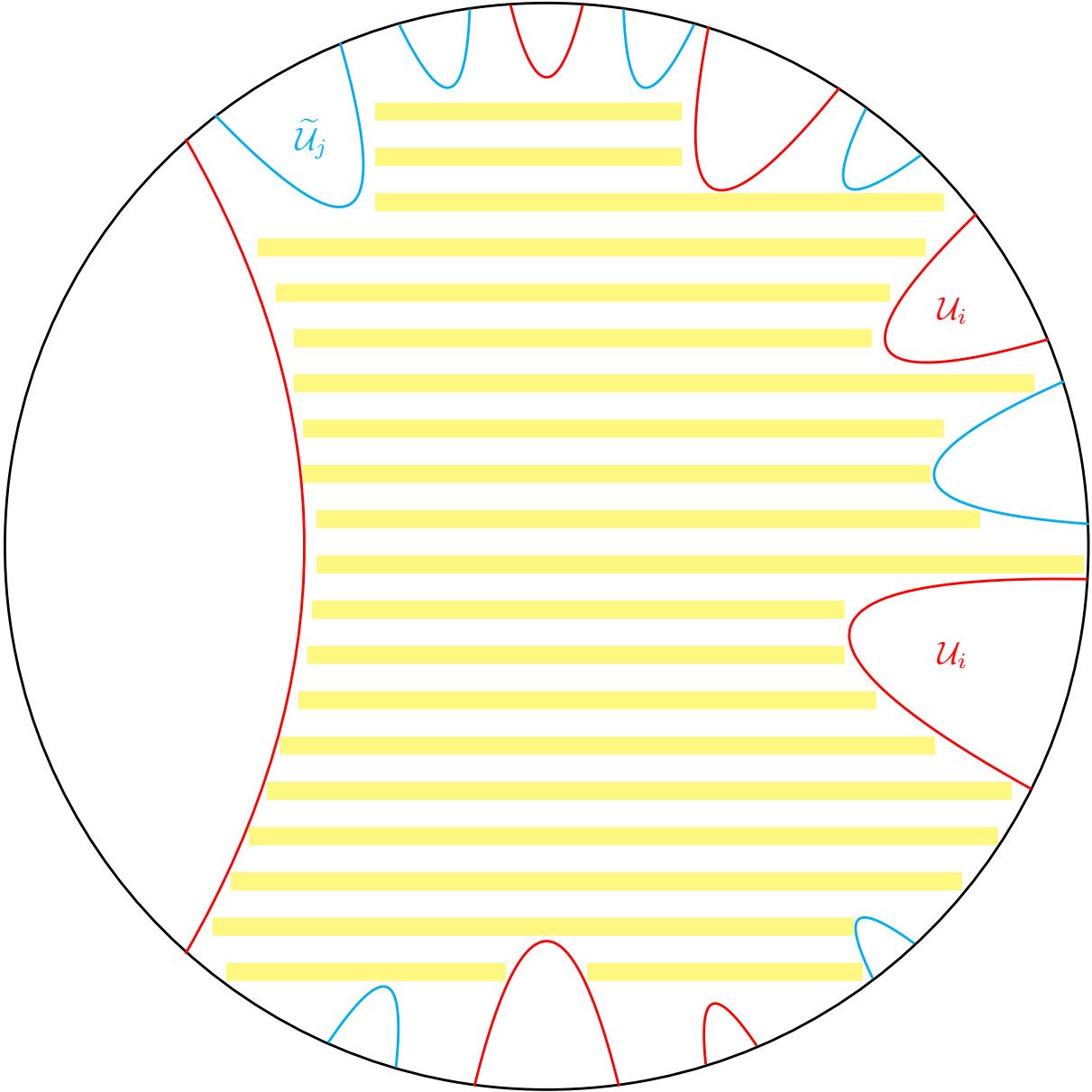


Figure 7.1: Davis complex Σ_{N_1} : 2-dimensional.

Remark 11. In Figure 7.1, the shaded part is the Davis complex Σ_{N_1} , with the interiors of red and blue regions u_i and \tilde{u}_j removed.

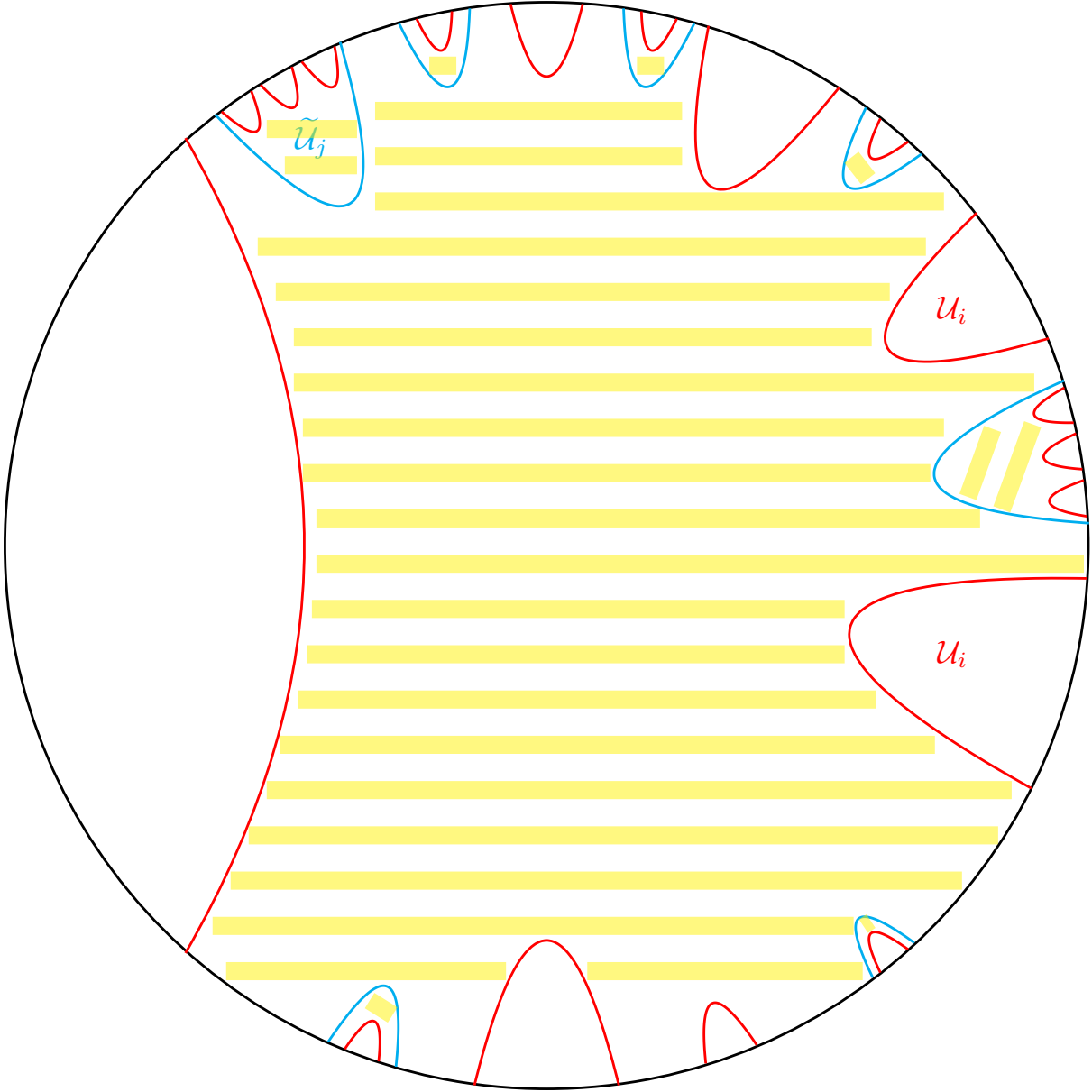


Figure 7.2: Davis complex Σ_{N_0} : 2-dimensional.

Remark 12. The shaded part is Σ_{N_0} , with all the red regions removed; in particular the red half-space in blue regions also needs to be removed. And $\Sigma_{N_1} \subseteq \Sigma_{N_0}$.

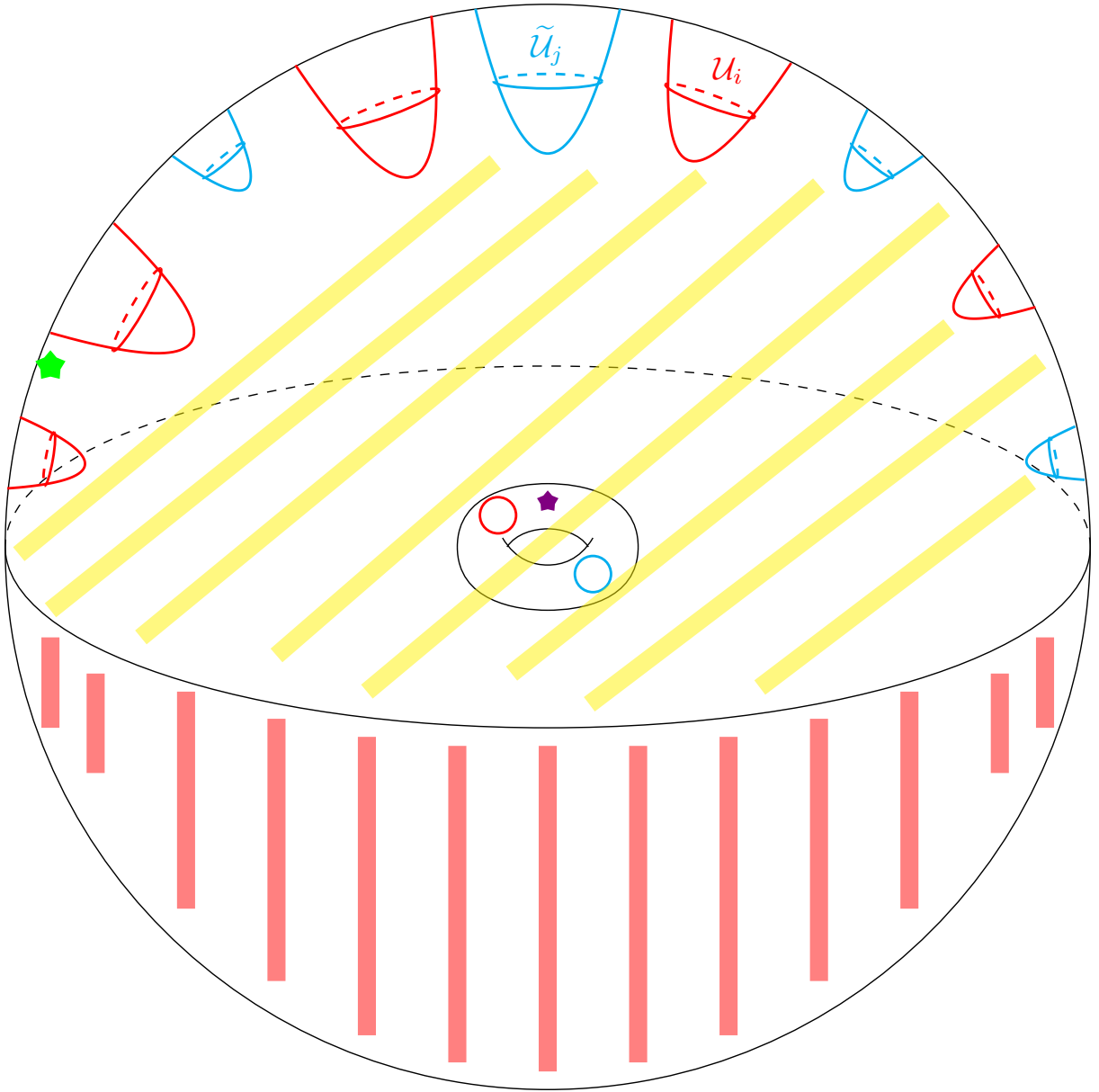


Figure 7.3: Davis complex Σ_{N_1} : 3-dimensional.

Remark 13. In Figure 7.3, the purple star represents the G_{non} graph lying in N_1 and the green star represents a nonplanar graph G_{non} lying in $\partial_\infty \Sigma_{N_1}$. And the red and the blue regions are removed.

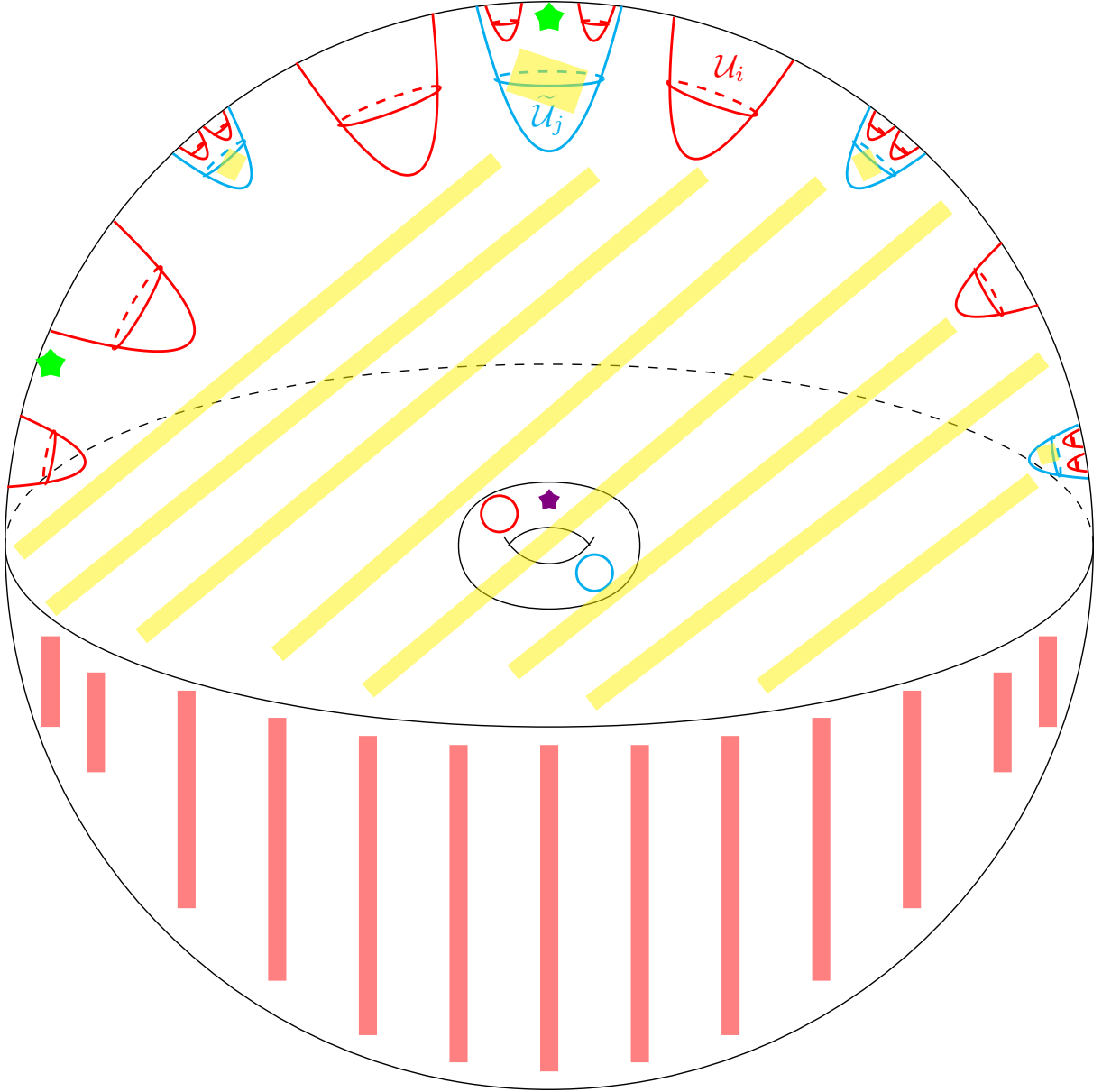


Figure 7.4: Davis complex Σ_{N_0} : 3-dimensional.

Remark 14. In Figure 7.4, all the red regions are removed, particularly, the red regions in the blue regions also need to be removed.

Chapter 8

No local cut point

In this chapter, we aim to prove $\partial_\infty \Sigma_{N_0}$ has no local cut point, i.e., for any neighborhood U of p_0 , there exists a neighborhood V' of p_0 such that $V' \subseteq U$ and each pair (q, r) in $(V' \setminus \{p_0\}) \setminus (\bigcup_{k=1}^{\infty} \mathring{B}_k)$ can be connected by a path l in $(U \setminus \{p_0\}) \setminus (\bigcup_{k=1}^{\infty} \mathring{B}_k)$, where B_k is defined shortly.

Our starting point is that the Pontryagin surface \mathcal{P} is locally path connected and has no local cut point. From this fact, we can always find a path l in $\mathcal{P} = \partial_\infty \Sigma_N$ connecting (q, r) , but l may go into the interiors of B'_k s (see Figure 8.1) which are not in $\partial_\infty \Sigma_{N_0}$ (We want to prove $\partial_\infty \Sigma_{N_0}$ has no local cut point). To do so, our strategy is to push the parts in the Pontryagin disks B'_k s to their boundaries (in our case they are circles). The process is described in Figure 8.4 and Figure 8.5. In one aspect, we should not push the path out of U , which can be guaranteed by Lemma 8.2.1. In another aspect, we need the “new path” to be continuous, especially when the path goes into and out of the B'_k s infinitely many times (oscillations). In order to prove this, we need the oscillation to be null, i.e., $\{C_{pq}\}$ is null (see Proposition 8.1.2), also the Pontryagin disk to be null which was derived in Chapter 6.

We split the proof into two cases, case 1: $p_0 \notin B_{k_0}$ for any k_0 and case 2: $p_0 \in B_{k_0}$ for some k_0 . For case 2, we need to deal with the special Pontryagin disk B_{k_0} where p_0 lies in.

To proceed, we need the following notations.

1. Let N be a flag triangulation of a closed surface, and denote $N_0 = N - a$.
2. Let $f : \mathbb{S}^1 \rightarrow S$ be a homeomorphism, \mathbb{S}^1 is the standard circle in \mathbb{R}^2 . See Figure 8.2.
 For any $p, q \in S$, denote by $p' = f^{-1}(p), q' = f^{-1}(q)$, $A_{p'q'} \cup B_{p'q'} = \mathbb{S}^1$, $A_{p'q'} \cap B_{p'q'} = \{p', q'\}$. Let $A_{p'q'}$ denote the shorter arc in \mathbb{S}^1 (if the arcs are of the same length, pick one of them), $A_{pq} = f(A_{p'q'})$ is the homeomorphic image of $A_{p'q'}$, i.e. $A_{pq} \approx A_{p'q'}$.
3. Denote the path segment between p and q in the Pontryagin disks B'_k s by I_{pq} .
4. Denote $C_{pq} := I_{pq} \cup A_{pq}$. See Figure 8.1.
5. Since the cardinality $\#\mathcal{T}_{N_0, a}$ is countably many, we can enumerate the Pontryagin disks removed as $\{B_k\}_{k=1}^\infty$;
 $B_k := \partial_\infty(g_k H_a^+)$, $g_k \in \mathcal{T}_{N_0, a}$; $\dot{B}_k := \partial_\infty(g_k H_a^+) \setminus \partial_\infty(g_k h_a)$. By proposition 5.2.1 B'_k s are disjoint.

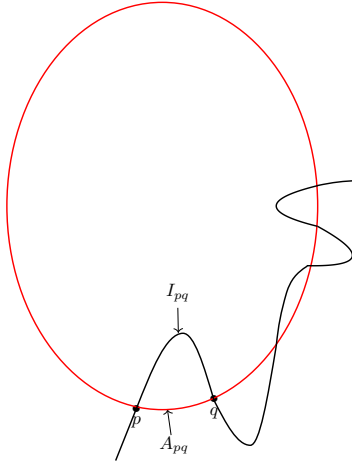


Figure 8.1: The path goes into and out of Pontryagin disk.

8.1 C_{pq} is null

In this section, we prove C_{pq} is null which is useful to verify that the “new path” after infinitely many times adjustments is continuous.

The proof of nullity of C_{pq} bases on that $\{A_{pq}\}$ and $\{I_{pq}\}$ are both null. For $\{A_{pq}\}$, we need the uniform continuity.

Fact 2. f is continuous, and \mathbb{S}^1 is compact, thus f is uniformly continuous, i.e. for any $\epsilon > 0$, there exists a $\delta > 0$, such that for every pair of points $y_0, y_1 \in \mathbb{S}^1$ with the metric inherited from \mathbb{R}^2 , $d_{\mathbb{S}^1}(y_0, y_1) < \delta$ implies $d_S(f(y_0), f(y_1)) < \epsilon$. So is f^{-1} .

Lemma 8.1.1. For any $\epsilon > 0$, there exists an $\tilde{\epsilon}$ such that $d(p, q) < \tilde{\epsilon}$ implies $\text{diam}A_{pq} < \epsilon$, where A_{pq} inherits the metric of the visual boundary. In particular, $\{A_{pq}\}_{p,q}$ is null.

Proof. By the uniform continuity of f , for any $\epsilon > 0$, there exists a $\delta > 0$, such that

$$d(x', y') < \delta \implies d(x, y) < \epsilon, \tag{8.1.1}$$

where $x' = f^{-1}(x), y' = f^{-1}(y)$.

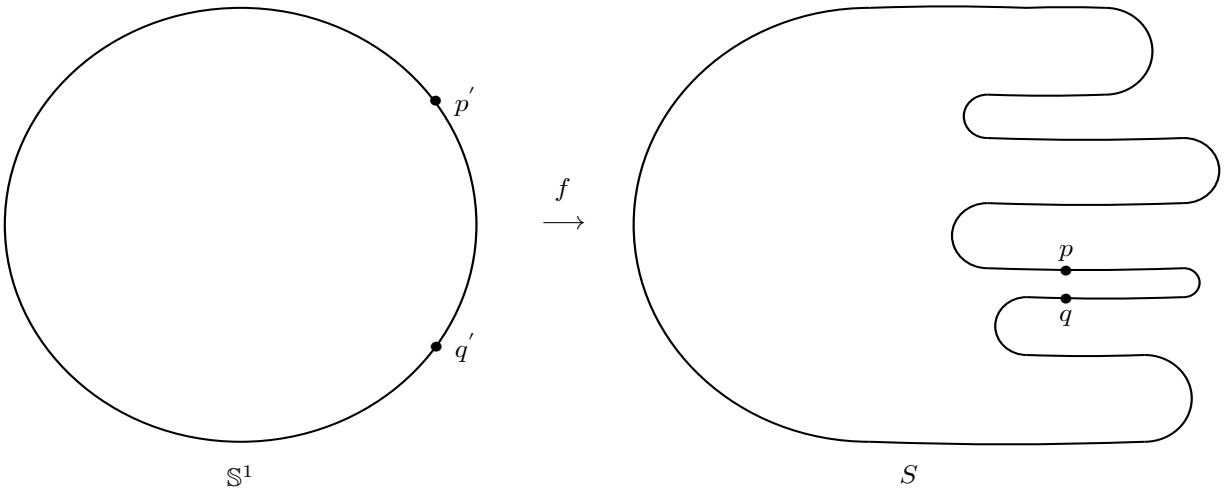


Figure 8.2: $\{A_{pq}\}_{p,q}$ is null.

By the uniform continuity of f^{-1} , for the chosen δ , there is an $\tilde{\epsilon}$ such that

$$d(p, q) < \tilde{\epsilon} \implies d(p', q') < \delta.$$

Note in S^1 , for any pair of points $x', y' \in A_{p'q'}$,

$$d(x', y') \leq d(p', q') < \delta.$$

By (8.1.1) and the arbitrariness of x' and y' , coupled with the fact that $A_{pq} \approx A_{p'q'}$, we deduce $\text{diam}A_{pq} < \epsilon$, see Figure 8.2.

□

Proposition 8.1.2. $\{C_{pq}\}_{p,q}$ is a null sequence.

Proof. Note $f^{-1}(\mathring{B}_k) = \bigcup_{i=1}^{\infty} \mathring{I}_i$, where I_i is null. $f(\partial I_i) \in \partial B_k$ and denote $f(\partial I_i)$ by $\{p_i, q_i\}$; denote $f(I_i)$ by I_{pq} and $\{I_{pq}\}_{p,q}$ is null.

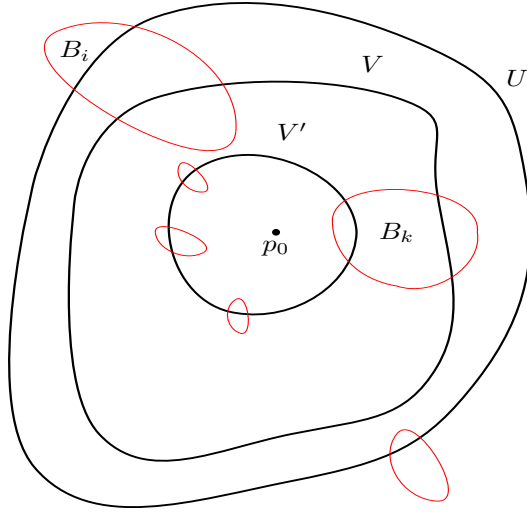
Note $\{I_i\}$ is a null sequence, and $\{d(p, q)\}_{p,q}$ is null as well, this implies $\{I_{pq}\}_{p,q}$ and $\{A_{pq}\}_{p,q}$ are both null sequences by the uniform continuity of f and Lemma 8.1.1, thus $\{C_{pq}\}_{p,q}$ is a null sequence. □

8.2 Small B_k inclusion

In what follows, we prove that we do not push the path out of U . This can be achieved by the following observation that for any $p_0 \in \partial_{\infty}\Sigma_{N_0}$, and any neighborhood $U \ni p_0$, the B'_k s near p_0 with small size will be contained in U , see Figure 8.3. More precisely, we have the following lemma.

Lemma 8.2.1. For any $p_0 \in U$, let $\delta > 0$ such that $B(p_0, \delta) \subseteq U$, and $V := B(p_0, \frac{\delta}{2})$, then for all B'_k s with $B_k \cap V \neq \emptyset$ and $\text{diam}(B_k) \leq \frac{\delta}{3}$, we have $B_k \subseteq U$.

Proof. The proof is immediate from the triangle inequality. □



- i) $\text{diam } B_k \leq \frac{\delta}{3}$
- ii) $\text{diam } B_i > \frac{\delta}{3}$
- iii) $B_k \subseteq U$

Figure 8.3: B'_k s with $\text{diam}(B_k) \leq \frac{\delta}{3}$ are included in U .

8.3 p_0 is not a local cut point

With the above preparation, now we are ready to prove the no local cut point property. We split the proof into two cases.

8.3.1 Case 1: $p_0 \in \mathcal{P} \setminus \bigcup_{k=1}^{\infty} B_k$

Proposition 8.3.1. *For any neighborhood U of p_0 , with $p_0 \notin B_k$ for any k , there exists a neighborhood V' of p_0 such that $V' \subseteq U$ and each pair (q, r) in $(V' \setminus \{p_0\}) \setminus (\bigcup_{k=1}^{\infty} \overset{\circ}{B}_k)$ can be connected by a path l in $(U \setminus \{p_0\}) \setminus (\bigcup_{k=1}^{\infty} \overset{\circ}{B}_k)$.*

Proof. We can take a Pontryagin disk V' such that $p_0 \in V' \subseteq V$, and $V' \cap B_k = \emptyset$ with $\text{diam}(B_k) \geq \frac{\delta}{3}$ (The number of B'_k s with $\text{diam}(B_k) \geq \frac{\delta}{3}$ is finite since $\{B_k\}$ is null).

For each pair (q, r) in $(V' \setminus \{p_0\}) \setminus (\bigcup_{k=1}^{\infty} \overset{\circ}{B}_k)$, they can be connected by a path l in V' since V' has no local cut point. But l may go into B'_k s (the interior of the red ball in Figure 8.4), which is not in $\partial_{\infty} \Sigma_{N_0}$.

To achieve our goal, we must push the path segments in B'_k s out. More precisely, we change the path segments from I_{pq} to A_{pq} . From Lemma 8.1.1, the new path can not go

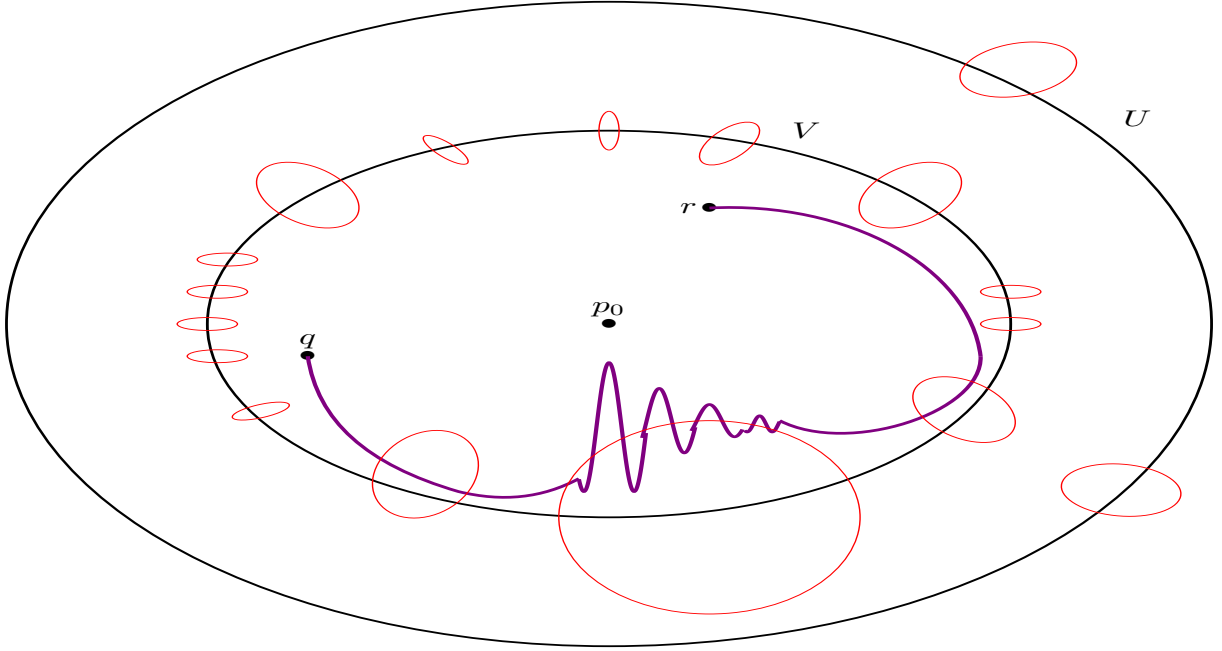


Figure 8.4: The purple path goes into the Pontryagin disks.

beyond U by the choice of V' .

Additionally, we need to justify the “new path” after these adjustments to be continuous. Thanks to the nullity properties of Proposition 8.1.2 and the fact $\{B_k\}_{k=1}^\infty$ is null from Proposition 6.2.6, we can prove that the “new path” is a real path as shown in Figure 8.5.

□

Infinitely many oscillations. The most involved situation is that the path goes in and out of the Pontryagin ball for infinitely many times, we call this phenomenon “oscillation”, see Figure 8.4

Step 1. Adjust the path in one Pontryagin disk.

Choose a strictly decreasing sequence $\{\delta_i\}_{i=1}^\infty$, i.e. $\delta_1 > \delta_2 > \delta_3 > \dots$, such that $\delta_i \rightarrow 0$ as $i \rightarrow \infty$.

Since $\{C_{pq}\}_{p,q}$ is null, either $diam(C_{pq}) > \delta_1$, or $\delta_{i+1} < diam(C_{pq}) \leq \delta_i$; and the number of oscillations between δ_{i+1} and δ_i is finite. Denote by g_0 the initial path before the adjustment, for the first stage, change the path segment I_{pq} in the Pontryagin disk to A_{pq} , where

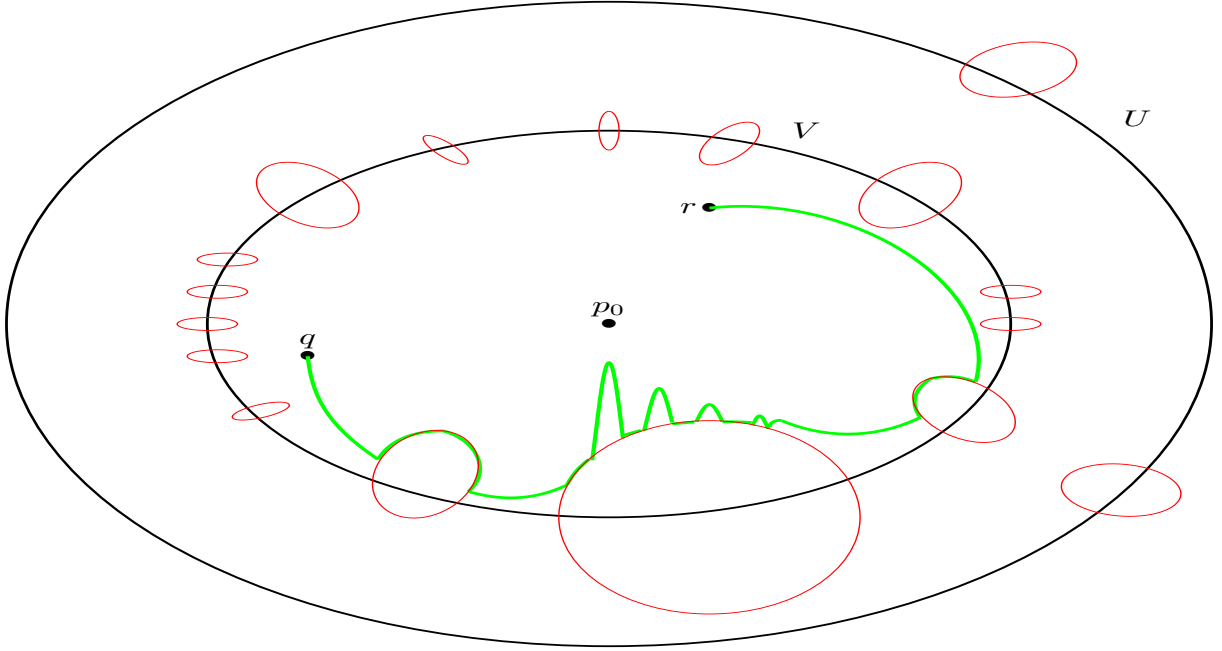


Figure 8.5: Push the path segments in B'_k s out.

Remark 15. After the push, the path would not go beyond U . The green path is the new one which lies in $\partial_\infty \Sigma_{N_0}$.

$diam(C_{pq}) > \delta_1$, and denote the resulting path by g_1 . Then at the i th stage change the path segment I_{pq} in the Pontryagin disk to A_{pq} with $\delta_{i+1} < diam(C_{pq}) \leq \delta_i$, denote the resulting path by g_i ; then we could repeat this process forever, and obtain a sequence $\{g_i\}_{i=1}^\infty$.

Claim 4. $\{g_i\}_{i=1}^\infty$ is a Cauchy sequence.

Proof. For any $\epsilon > 0$, take an N such that $\delta_N < \epsilon$ (since $\delta_i \rightarrow 0$), then for $n, m > N$, we have $d(g_n, g_m) \leq \delta_{m+1} < \delta_N < \epsilon$. □

By Claim 4, we are ready to conclude that the limit of $\{g_i\}_{i=1}^\infty$ is a continuous path.

Step 2. Adjust the path in all of the Pontryagin disks.

Now we can use the similar trick as above, choose a strictly decreasing sequence $\{\epsilon_i\}_{i=1}^\infty$, i.e. $\epsilon_1 > \epsilon_2 > \epsilon_3 > \dots$, such that $\epsilon_i \rightarrow 0$ as $i \rightarrow \infty$.

By nullity property, we have $\{diam(B_k)\}$ is null, either $diam(B_k) > \epsilon_1$, or $\epsilon_{i+1} < diam(B_k) \leq \epsilon_i$ for some i ; and the number of Pontryagin disks with diameter between ϵ_{i+1} and ϵ_i is finite.

Denote by f_0 the initial path before the adjustment, for the 1st stage, change the path segments in the Pontryagin disks with diameter greater than ε_1 as above; and denote the resulting path by f_1 ; repeat this process, generally, at the i th stage, we change the path segments in the Pontryagin disks with $\varepsilon_{i+1} < \text{diam}(B_k) \leq \varepsilon_i$, denote the resulting path by f_i , then we obtain a sequence $\{f_i\}_{i=1}^\infty$.

Claim 5. $\{f_i\}_{i=1}^\infty$ is a Cauchy sequence.

Proof. For any $\epsilon > 0$, take an N such that $\varepsilon_N < \epsilon$ (since $\varepsilon_i \rightarrow 0$), then for $n, m > N$, we have $d(f_n, f_m) \leq \varepsilon_{m+1} < \varepsilon_N < \epsilon$. \square

By Claim 5, there exists a limit f of $\{f_i\}_{i=1}^\infty$ and f is a path. Let f be denoted by l' , the proof is completed.

8.3.2 Case 2: $p_0 \in B_{k_0}$ for some k_0

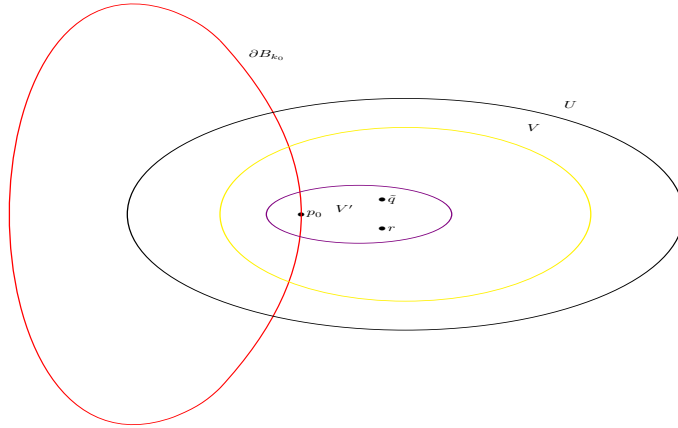


Figure 8.6: Case 2: $p_0 \in \partial B_{k_0}$.

Proposition 8.3.2. For any neighborhood U of p_0 in \mathcal{P} , where $p_0 \in \partial B_{k_0}$ for some k_0 , there exists a neighborhood V' of p_0 such that $V' \subseteq U$ and each pair (\tilde{q}, r) in $(V' \setminus \{p_0\}) \setminus (\bigcup_{k=1}^\infty \mathring{B}_k)$ can be connected by a path l in $(U \setminus \{p_0\}) \setminus (\bigcup_{k=1}^\infty \mathring{B}_k)$.

Proof. Take V to avoid B'_k s with $\text{diam}(B_k) > \frac{\delta}{3}$ (possibly except B_{k_0}) $k \neq k_0$ as in Lemma 8.2.1. Note there exists a map f such that $f(B_{k_0}) = \mathcal{P} \setminus B_{k_0}$ fixing ∂B_{k_0} . Take a small enough Pontryagin disk $V' \ni p_0$ such that $f(V') \subseteq V$, as shown in Figure 8.6. For any pair of point (\tilde{q}, r) in $(V' \setminus \{p_0\}) \setminus (\bigcup_{k=1}^{\infty} \mathring{B}_k)$, note V' has no local-cut point, $\forall p, q \in V' \cap S$, there is a path l connecting p and q , such that $l \subseteq V'$ and $p_0 \notin l$. See Figure 8.7.

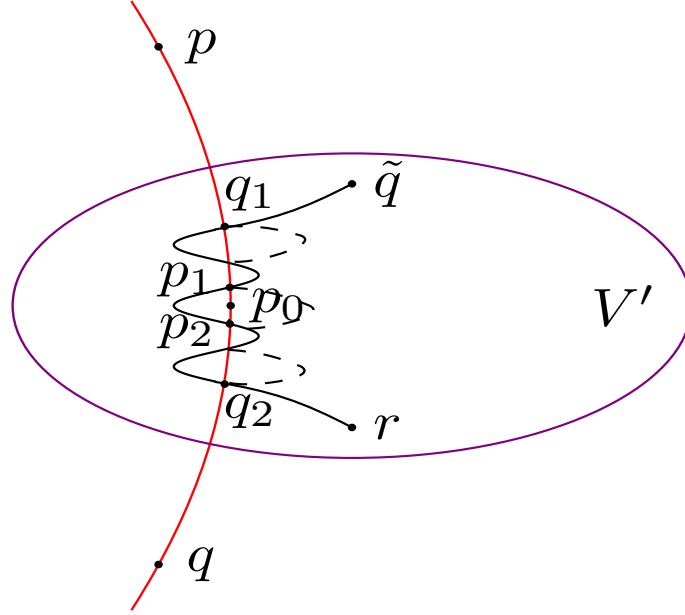


Figure 8.7: Reroute the path l .

Let $C = l^{-1}(B_{k_0})$ and $D = l^{-1}(P \setminus \mathring{B}_{k_0})$ closed subsets of $[0, 1]$ such that $C \cap D = \{t \mid l(t) \in S\}$.

Define $\tilde{l} : [0, 1] \rightarrow \mathcal{P}$ by

$$\tilde{l}(t) = \begin{cases} l(t), & \text{if } t \in D, \\ f \circ l(t), & \text{if } t \in C. \end{cases}$$

Denote the modified path by \tilde{l} , repeat the process in Proposition 8.3.1 to push the segment in B'_k s with $\text{diam}(B_k) \geq \frac{\delta}{3}$ onto the ∂B_k , denote the new path by l' , this completes the case 2. □

Chapter 9

Other properties of $\partial_\infty \Sigma_{N_0}$

Now we turn to verify the other properties of $\partial_\infty \Sigma_{N_0}$.

9.1 Path connected and locally path connected

The following propositions are completely similar repetitions of process to prove the no local cut point, see Proposition 8.3.1, so we omit the proofs.

Proposition 9.1.1. *For any pair $(p, q) \in \mathcal{P} \setminus \left(\bigcup_{k=1}^{\infty} \mathring{B}_k \right)$, there exists a path connecting them in $\mathcal{P} \setminus \left(\bigcup_{k=1}^{\infty} \mathring{B}_k \right)$.*

Proposition 9.1.2. *For any neighborhood U of p_0 in \mathcal{P} , where $p_0 \in \mathcal{P} \setminus \left(\bigcup_{k=1}^{\infty} \mathring{B}_k \right)$, there exists a neighborhood V' of p_0 such that $V' \subseteq U$ and each pair (q, r) in $V' \setminus \left(\bigcup_{k=1}^{\infty} \mathring{B}_k \right)$ can be connected by a path ℓ in $U \setminus \left(\bigcup_{k=1}^{\infty} \mathring{B}_k \right)$.*

9.2 Visual boundary is 1-dimensional

On the one hand, $\dim \partial_\infty W_{N_0} = \max\{n : \tilde{H}^n(N_0) \neq 0 \text{ or } \tilde{H}^n(N_0 \setminus \Delta) \neq 0 \text{ for some simplex } \Delta \subseteq N_0\}$ (where \tilde{H}^* denotes the reduced cohomology) (proof of Lemma 2.5 [30]). Since N_0 and $N_0 \setminus \Delta$ are both homotopy equivalent to bouquets of circles, we have $\tilde{H}^2(N_0) = 0$,

or $\tilde{H}^2(N_0 \setminus \Delta) = 0$, for any simplex $\Delta \subseteq X$, i.e. $\dim \partial_\infty W_{N_0} \leq 1$. On the other hand, $\dim \partial_\infty W_{N_0} \geq 1$ since it contains a subset homeomorphic to the circle S^1 . Thus $\dim \partial_\infty W_{N_0} = 1$.

9.3 Completion of the main theorem

Combining with Proposition 7.2.2, Proposition 8.3.1, and Proposition 8.3.2, we complete the proof of Theorem 1.1.1.

Chapter 10

Closing comments and open questions

It is worthy to mention that our methods can be applied to the high dimensional case which needs to be investigated further. Exploiting the method applied in 2-dimensional case, we can also get the following theorem which allows us to expand upon the work of Lafont-Tshishiku [23].

Recall that the homology sphere is a closed manifold with the same homology as S^n ; the homology ball can be obtained by removing a single vertex from a triangulated homology sphere. A Jakobsche space and a Jakobsche ball are higher dimensional analogues of the Pontryagin surface and Pontryagin disk respectively. I expect to be able to prove: there exist infinitely many different Gromov boundaries for hyperbolic aspherical 4-manifold groups.

However, there are numerous questions left unanswered. The following is a special case of a conjecture due to Świątkowski-Zawiślak [34].

Conjecture 10.0.1. *Let K be a flag triangulation of a closed manifold, K_0 a subcomplex obtained by removing a single vertex, and W_0 be the Coxeter group with nerve K_0 , then the $CAT(0)$ boundary of W is homeomorphic to $\mathcal{X}^r(K_0)$.*

A positive answer to Conjecture 10.0.1 will allow us to solve:

Conjecture 10.0.2. *For each homology 3-sphere H^3 , there exists an aspherical 4-manifold M^4 with boundary such that $\pi_1(M^4)$ is hyperbolic and the Gromov boundary of $\pi_1(M^4)$ is the*

Sierpinski-Jakobsche space $\mathcal{X}^r(H_0^3)$. (See [34] for a precise definition.)

BIBLIOGRAPHY

- [1] P. Abramenko and K. Brown. *Buildings: Theory and Applications*. Springer, 2008.
- [2] R. D. Anderson. A characterization of the universal curve and a proof of its homogeneity. *Annals of Mathematics* 67 (2):313-324, 1958.
- [3] R. D. Anderson. One-dimensional continuous curves and a homogeneity theorem. *Annals of Mathematics* 68 (1):1-16, 1958.
- [4] A. Bartels, W. Lück, and S. Weinberger. On hyperbolic groups with spheres as boundary. *Journal of Differential Geometry* 86 (1):1-16, 2010.
- [5] M. R. Bridson and A. Haefliger. *Metric space of non-positive curvature*. Springer-Verlag, Berlin, 1999.
- [6] F. Dahmani, V. Guirardel, and P. Przytycki. Random groups do not split. *Mathematische Annalen* 349 (3): 657-673, 2011.
- [7] D. Danielski. Right-angled Coxeter groups with Menger curve boundary. *Bulletin of the London Mathematical Society* 54 (3): 977-995, 2022.
- [8] D. Danielski and J. Świątkowski. A note on the complete characterizations of hyperbolic Coxeter groups with Sierpiński curve boundary and with Menger curve boundary. *arXiv:2110.01922*, 2023.
- [9] R. J. Daverman and T. L. Thickstun. Degree-one, monotone self-maps of the pontryagin surface are near-homeomorphisms. *Pacific Journal of Mathematics* 303 (1): 93-131, 2019.
- [10] M. Davis. Groups generated by reflections and aspherical manifolds not covered by Euclidean space. *Mathematische Annalen* 117 (2): 93-131, 1983.
- [11] ———. *The Geometry and Topology of Coxeter Groups*. London Mathematical Society Monograph Series, Princeton University Press, 2008.
- [12] A. N. Dranishnikov. Boundaries of Coxeter groups and simplicial complexes with given links. *Journal of Pure and Applied Algebra* 137 (2): 139-151, 1999.

- [13] H. Fischer. Boundaries of right-angled Coxeter groups with manifold nerves. *Topology* 42 (2): 423-446, 2003.
- [14] ———. Visual boundaries of right angled Coxeter groups and reflection manifolds. *Dissertation, The University of Wisconsin-Milwaukee*, 1998.
- [15] C. Guilbault, M. Moran, and C. Trel. Boundaries of Baumslag-Solitar groups. *Algebraic and Geometric Topology* 19 (4): 2077-2097, 2019.
- [16] A. Gagarin and W. Kocay. Embedding graphs containing K_5 -subdivisions on the torus. *Journal of Combinatorial Mathematics and Combinatorial Computing* 80: 207-223, 2012.
- [17] A. Gagarin and W. Kocay. Embedding K_5 and $K_{3,3}$ on orientable surfaces. *Discrete Applied Mathematics*: <https://doi.org/10.1016/j.dam.2023.05.018>., 2023.
- [18] M. Haulmark. Boundary classification and 2-ended splittings of groups with isolated flats. *Journal of Topology* 11 (3): 645-665, 2018.
- [19] M. Haulmark, G. C. Hruska, and B. Sathaye. Nonhyperbolic Coxeter groups with Menger boundary. *L'Enseignement Mathématique* 65 (1-2): 207-220, 2019.
- [20] W. Jakobsche. Homogeneous cohomology manifolds which are inverse limits. *Fundamenta Mathematicae* 137 (2):81-95, 1991.
- [21] M. Kapovich and B. Kleiner. Hyperbolic groups with low-dimensional boundary. *Annales Scientifiques de l'É. N.S. 4^e série* 33 (5):647-669, 2000.
- [22] F. Dahmani, V. Guirardel, and P. Przytycki. Random groups do not split. *Mathematische Annalen* 349 (3):657-673, 2011.
- [23] J-F Lafont and B. Tshishiku. Hyperbolic groups with boundary an n-dimensional Sierpinski space. *Journal of Topology and Analysis* 11 (01):233-247, 2019.
- [24] W. J. R. Mitchell, D. Repovš, and E.V. Ščepin. On 1-cycles and the finite dimensionality of homology 4-manifolds. *Topology* 31 (3): 605-623, 1992.
- [25] G. Moussong. Hyperbolic Coxeter groups. *Dissertation (Ph.D.)-The Ohio State University*, 1988.
- [26] J. R. Munkres. *Elements of Algebraic Topology*. Addison Wesley Publishing Company, 1984.
- [27] J. R. Stallings. On torsion-free groups with infinitely many ends. *Annals of Mathematics* 88 (2): 312-334, 1968.
- [28] M. Ronan. *Lectures on Buildings*. Academic Press, INC, 1989.

- [29] J. Świątkowski. Trees of manifolds as boundaries of spaces and groups. *Geometry & Topology* 24 (2): 593 - 622, 2020.
- [30] ———. Hyperbolic Coxeter groups with Sierpiński carpet boundary. *Bulletin of the London Mathematical Society* 48 (4):708-716, 2016.
- [31] P. Scott and T. Wall. *Homological Group Theory*. London Mathematical Society Lecture Note Series 36, Cambridge University Press, 1979.
- [32] A. Thomas. *Geometric and Topological Aspects of Coxeter Groups and Buildings*. Nachdiplomvorlesung an der ETH Zürich im FS, 2016.
- [33] D. Wise. *From Riches to Raags: 3-Manifolds, Right-Angled Artin Groups, and Cubical Geometry*. American Mathematical Society, 2012.
- [34] P. Zawisłak. Trees of manifolds with boundary. *Colloquium Mathematicum* 139 (1):1-24, 2015.
- [35] ———. Trees of manifolds and boundaries of systolic groups. *Fundamenta Mathematicae* 207 (1):71-99, 2010.